Electric Vehicle Charging Station Resource Allocation: A Data-Driven Robust Optimization Approach

by

Mohammadhadi Rouhani

A thesis submitted in partial fulfillment of the requirements for the degree of

Master of Science

Department of Computing Science

University of Alberta

Abstract

The adoption of electric vehicles has been growing steadily in recent years, and projections indicate that this trend will continue. However, the availability and capacity of charging stations have not kept pace with this growth, leading to long wait times and congestion at charging stations. The installation and operation of electric vehicle charging stations (EVCSs) are non-trivial problems and require careful consideration of several factors, including the size of the charging station. This involves determining the optimal number of charging units and their capacity to meet the expected charging demand. This becomes even more complex when the charging station is coupled with an on-site solar photovoltaic (PV) panel system and a battery energy storage system (BESS).

The goal of sizing EVCSs is to create a methodology that can enhance the utilization of charging infrastructure, decrease waiting times, and enhance the user experience. An efficient sizing strategy will guarantee that the charging stations can meet the projected demand while keeping installation and operating expenses to a minimum. Moreover, the proper implementation of charging infrastructure is crucial to the widespread adoption of EVs, as the availability of charging infrastructure is a key factor in consumer decision-making.

We study two problems in this thesis:

Our first task involves a two-stage sizing assessment of a single EVCS that is co-located with on-site PV and BESS systems. Initially, we want to identify EVCS sizing options that meet a blocking rate threshold, which is a user experience performance metric. Subsequently, for each optimal-sized EVCS option, we recommend robust sizing solutions for the PV and BESS systems to minimize the reliance on the main power grid. We address this problem using convex optimization and introduce a Chebyshev inequality for robust sizing. Our simulation results establish a correlation between the sizing of the PV and BESS systems and confirm that larger sizing of PV and BESS is required for reduced dependency on the main grid. Additionally, we discover that a significant PV system is necessary for an EVCS to rely entirely on solar energy without the assistance of a BESS. Thus, we recommend combining a PV system with a BESS for optimal performance.

In the second problem, we proceed to assess a network of EVCSs and establish an optimization problem to optimally size each EVCS in the network, subject to various constraints. These constraints stem from performance metrics (such as response time) and total costs, encompassing both capital and operating costs, across all locations. Due to the complex nature of this queueing system optimization problem, we must make certain assumptions to obtain a feasible solution. We solve the optimization problem for a small-scale network of EVCSs including the traffic flow. Our findings indicate that when optimizing a network of EVCSs, the sizing alternative at each location is likely to have a

direct impact on the performance metrics.

To Samira, Amirali & Nika

Acknowledgements

[*Be sure we shall test you with something of fear and hunger, some loss in goods, lives, and the fruits of your toil. But give glad tidings to those who patiently persevere.*][1]

My utmost gratitude goes to God, who has blessed me with the strength and hope to finish this research work. His ultimate kindness and compassion have showered me with glory and mercy.

I express my gratitude to Dr. Omid Ardakanian and Dr. Petr Musilek, my supervisors, for their invaluable advice and guidance during this research work.

My family has been a constant source of love, patience, and support throughout this challenging period, and I am incredibly fortunate to have them by my side. Pursuing a graduate degree in Computing Science during the pandemic was a formidable task, and it involved numerous sleepless nights spent meeting deadlines. Nevertheless, Samira's unwavering support has been invaluable, and it helped me stay focused on my goals and forge ahead on this path to success. I will always cherish her presence in my life.

---

[1]Quran, 2:155

Contents

List of Tables

List of Figures

Glossary of Terms

Abbreviation	Full Form
ACN	adaptive charging network
BCMP	Baskett, Chandy, Muntz, and Palacios
BESS	battery energy storage systems
CS	charging station
CTMC	continuous-time Markov chain
DC	direct current
DCFC	DC fast charger
DEA	data envelopment analysis
DER	distributed energy resources
EV	electric vehicles
EVCS	electric vehicle charging station
HEV	hybrid electric vehicles
ILP	integer linear programming
MILP	mixed integer linear programming
MLE	maximum likelihood estimation
MVA	mean value analysis

Abbreviation	Full Form
PASTA	Poisson arrivals see time averages
PHEV	plug-in hybrid electric vehicles
PEV	plug-in electric vehicles
PV	photovoltaic
RES	renewable energy sources
RUL	ratio of unmet load
QoS	quality of service

Variable	description
$\mu^{(s)}$	service rate at sth charger pod
n_{Li}	number of level i charger
λ	arrival rate at a charging station
$P_L(s)$	active power consumed at a charging station in state s
$\bar{P}_{Li}$	active power rating for level i charger
η_i	charging efficiency for level i charger
π_{blk}	blocking probability
$\bar{P}_G$	grid active power capacity for an EVCS
E_B	BESS energy capacity [kWh]
$\mathcal{E}_B$	set of feasible BESS capacity (E_B)
$\mathcal{H}$	set of feasible tuples of number of charger pods
$\mathcal{T}_i$	tuple of feasible number of level 2 and level 3 charger pods
T	sizing optimization time horizon
P_{in}^i	power supplied to the EVCS from solar panel at time i
e_b^i	energy stored in battery at time i
P_c, P_d	battery charge, discharge rate
δ	maximum proportion of charging demand supplied by the main grid
α_c, α_d	charge and discharge correction factors
P_{cs}^i	EVCS charge demand at time i
S^i	solar energy produced at time i
C_{pv}	kW solar capacity installed at EVCS site
C_{pv}^*	optimal solar capacity
T_u	time resolution for the optimization time horizon T
e^i	amount of energy to be supplied by the main grid

Variable	description
N_{pv}	Total number of samples drawn for random variable C_{pv}
$m_{C_{N_{pv}}}$	mean of solar capacity with N_{pv} number of samples
$\sigma_{C_{N_{pv}}}$	standard deviation of solar capacity with N_{pv} number of samples
γ	confidence factor coefficient of the Chebyshev inequality
$\pi_{n_1,n_2,...,n_k}$	limiting probability of a charging station network at $n_1, n_2,..., n_k$ state
n_{Li}	number of level i charger
M_{ev}	EV population of a network of EVCS
$\mathbb{E}[x]$	expected value of random variable x
$N_j^{(M)}$	number of EVs at j^{th} station with total M population
$T_j^{(M)}$	response time of an EV at j^{th} station with total M population
$\lambda^{(M)}$	Total EV arrival rate in a closed EVCS network with population M
$f_{c_j}(k_j, \mu_j)$	cost function of jth EVCS with k_j chargers at μ_j service rate
P_{Tr_i}	transformer active power capacity at i^{th} EVCS location
τ	sum of maximum tolerable average response times at N EVCS
N	Number of charging stations in a closed EVCS network
k_i^{max}	maximum number of chargers being installed at i^{th} EVCS

Chapter 1

Introduction

Electric vehicles (EVs) have gained immense popularity in recent years as an environmentally-friendly alternative to gasoline-powered vehicles. The transition from internal combustion engine vehicles to fully electric vehicles promises a tremendous reduction in CO_2 emissions and improved air quality [1]. The technological achievements in the EV manufacturing field (e.g. increased driving range, reduced charging time, low on parts compared to gas-based vehicles) have triggered a spike in demand for EVs. By 2040, 57% of all passenger vehicles are projected to be electric worldwide. One of the critical components of this electric-based transportation infrastructure is the electric vehicle charging stations (EVCS). An EVCS typically consists of multiple charging pods which may have different types of chargers. The proper sizing and allocation of chargers at EVCSs are crucial for the efficient and cost-effective operation of the charging infrastructure.

Oversized EVCSs can lead to underutilization, which means the charging infrastructure is not being used efficiently. On the other hand, undersized EVCSs can lead to long wait times, frustrated customers, and ultimately, lost revenue for the charging station operators. Therefore, the sizing of EVCSs should be based on the expected demand for charging services, which can vary significantly depending on various factors such as the location of the charging

station, time of day, day of the week, and season. There are heterogeneous types of chargers based on their rating charge power (level 1, 2, and 3 (or fast DC)) and this makes the sizing problem more difficult to solve. Hence we focus our concentration more on determining the efficient number of chargers for both single and multiple EVCS locations.

Throughout this thesis, our goal is to find answers to the following research questions:

- What is the optimal sizing strategy for EVCSs with on-site PV and BESS systems to enhance the utilization of charging infrastructure, decrease waiting times, and enhance the user experience?

- How can a network of EVCSs be optimally sized while ensuring performance metrics and total costs are within acceptable limits?

Several approaches have been introduced in the literature to properly size an EVCS located in a certain area of the city. In chapter 2, we provide a comprehensive survey of the existing strategies on

- factors that must be considered when sizing an EVCS (e.g. EV user range anxiety and satisfaction, service provider profit, transformer feeder capacity, etc.).

- suitable strategies for sizing an EVCS, even when it is co-located with renewable energy sources including solar panels and battery storage systems.

In Chapter 3, we focus on presenting fundamental concepts of queueing theory that play a crucial role in creating a model for EV charging workload and defining the sizing problem. Our discussion delves into the modeling of EV workload at EVCS and showcases the reliability of these models by incorporating actual datasets from real-world scenarios.

In Chapter 4, we present a two-stage approach to optimize the sizing of a single charging station, which is co-located with a solar panel and battery storage system. Our optimization focuses on two primary objectives: 1) identifying the optimal number of charger ports that can meet a pre-determined threshold on blocking probability at the EVCS (i.e. EVCS sizing), and 2) providing a reliable sizing recommendation for the renewable energy system to minimize reliance on the main power grid based on the EVCS's sizing. We explain in this chapter the robustness of our approach which stems from:

- future EV demand growth

- seasonal/daily stochastic changes solar power generation

- EVs time of charging throughout an optimization time horizon

The independent operation of an EVCS can significantly reduce carbon emissions and offer several environmental benefits. To achieve these objectives, we propose a novel CTMC based on the EVCS states, leveraging queueing theory. Additionally, we introduce two different types of charger ports. To ensure a robust sizing option, we utilize Chebyshev's inequality to establish confidence criteria for the reliability of the sizing strategy. Chapter 4 can be summarized schematically in Figure 1.1 (from left to right).
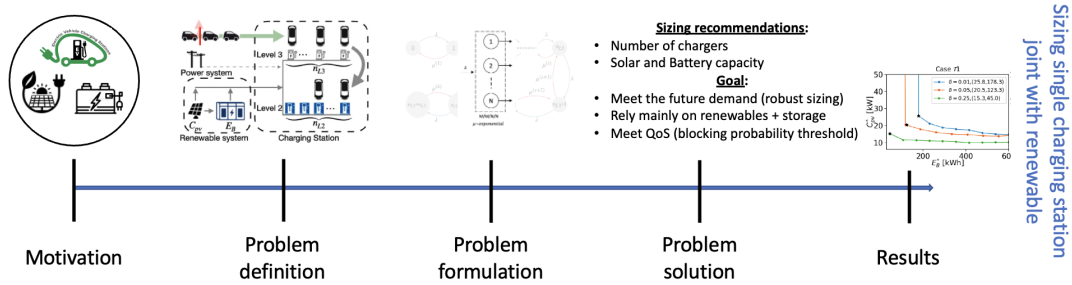
Figure 1.1: (from left to right) Demographic summary of Chapter 4

In Chapter 5, we focus on presenting sizing strategies for multiple charging stations in a network, such as a road network. Our discussion includes incorporating a traffic network with infinite size capacity, modeling distributed EVCSs,

and formulating an optimization problem to determine the sizing of multiple charging stations. We solve this optimization problem for a small-scale case study and demonstrate the effectiveness of the proposed sizing strategy for a network of EVCS. This chapter can be summarized in the demographic shown in Figure 1.2 (from right to left).
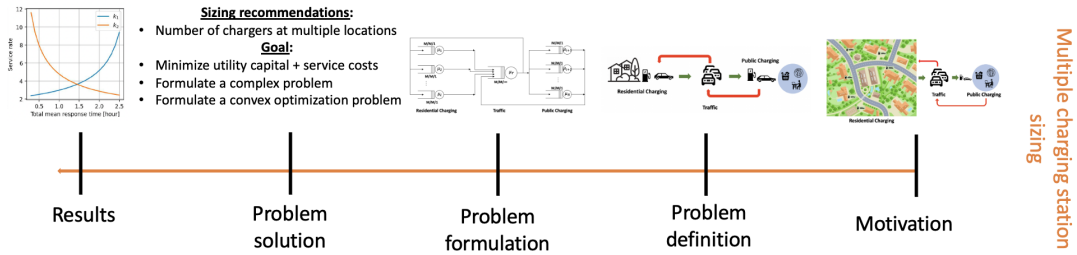
Figure 1.2: (from right to left) Demographic summary of Chapter 5

Chapter 6 provides concluding remarks and summarizes the research outcomes and our findings around EVCS sizing strategies.

Chapter 2

Literature Review

In the past decade, there was a spike in the demand for EVs and it is anticipated that this demand will grow at an unprecedented rate in the future. Designing and analyzing the charging infrastructure for EVs goes back to when the first fast charging equipment was developed by SatCon in 1994 [2]. The company then investigated Rapid-recharge projects at levels of approximately 150 kW for blue bird bus vehicles. There has been a growing demand to charge at the residential premise and so different types of chargers emerged. According to an article, the electrification of U.S. transportation is expected to raise demand by 800-1700 TWh/year by the 2050s, which accounts for 21-44% of the entire electricity demand in the U.S. in 2016 [3]. The main concern is whether the traditional expansion of generation capacity can meet this surge in demand. Additionally, addressing the spatio-temporal patterns of electricity demand from EV charging poses a complementary challenge [4].

Our goal in this chapter is to review the literature on the following topics:

- EVCS Planning & Operation Optimization Goals

- Sizing of charging stations jointly with solar panel and battery storage

In summary, the literature on sizing strategies, operation, and planning optimization for charging stations has identified several key concerns that need

to be addressed for the successful deployment and operation of EVCSs. These concerns include range anxiety, investment, service costs, location, expansion planning, and grid constraints on transformer capacity. By addressing these issues, policymakers, and stakeholders can promote the widespread adoption of EVs and accelerate the transition toward a sustainable transportation system.

Some key goals in adopting joint sizing of EVCS and solar PV panels are summarized in Table 2.1. Table 2.2 brings a summary review of EVCS networks.

2.1 EVCS Planning & Operation as An Optimization Problem

The increasing adoption of EVs has led to a growing demand for EVCSs. As a result, research in sizing strategies, operation, and planning optimization for EVCSs has gained significant attention in recent years. Key concerns in the literature that need to be solved for the deployment and operation of EVCSs include range anxiety, investment, and service costs, location and expansion planning, and grid constraints on transformer capacity.

The first work on analyzing the sizing of EVCS was initiated in 2010 to study the optimal design of fast EVCS [20]. The authors analyzed an optimal design considering the topology and technology of various power electronics converters.

2.1.1 Adopting Queueing Theory Models

Queueing theory is a powerful tool that can be used to optimize the performance of EVCSs. It is crucial to accurately size these charging stations to ensure that they can meet the increasing demand while minimizing wait times and maintaining high levels of service quality. Queueing theory models provide a

Table 2.1: Summary of literature review on joint sizing of EVCS and solar PV panels

| Ref | Modeling | | Goal |
	EVCS	Renewables	
[5]	Simplified Erlang Loss model	PV and BESS Dynamics	minimize net investment and maintenance costs
[6]	Erlang B model (M/M/c/c)	Wind, PV, and BESS	maximize net present value (i.e. EVCS service provider profit)
[7]	model EVCS feeder as M/M/1	N/A	optimize service capacity and arrival rate for a given EVCS capacity
[8]	Dual mode Queueing Model	N/A	minimize service drop rate
[9]	Simplified model	scheduling of PV and BESS	minimize energy loss of distribution grid
[10]	regression model for M/M/c	N/A	find a trade-off between total investment cost minimization and customer satisfaction
[11]	M/M/c	PV panels and BESS	minimize the number of charging ports while maintaining the waiting time within a permissible threshold
[12]	M/M/c/k/N	PV panels and wind farms	find a probabilistic model for power grid characteristics
[13]	the modified capacitated-flow refueling location model	integrated PV generation with voltage control capability	minimize the cost of charging and upgrading and expansion costs of the grid

rigorous approach to sizing EV charging stations by taking into account the stochastic nature of EV arrivals and service times. These models can provide insights into the optimal number of charging stations, the optimal service rate, and the expected wait times.

Table 2.2: Summary of literature review on optimization goals for EVCS networks

Ref	EVCS Modeling	Goal
[14]	multi-server network of M/M/c	Analyze dynamic responsive price adjustment
[15]	network of M/M/c/c	minimize blocking probability, maximize profit by hard limiting the maximum charging delivery
[16]	joint distribution system and a network of M/M/g/z EVCS	maximal usage of charger ports at each EVCS through a dynamic programming allocation
[17]	BCMP network of EVCS and traffic	charging decision making mechanism to balance load at EVCSs
[18]	closed Jackson's network	investment minimization cost
[19]	mixed queueing network for battery swapping modeling M/M/S/N	Blocking probability evaluation

Empirical evidence from the literature suggests that queueing models have been effective in sizing EV charging stations. For example, a study conducted by Zhang et al [21] used a queueing model to optimize the performance of a DC fast charging station. The study found that increasing the number of charging stations and reducing the service time can significantly reduce wait times and increase the utilization rate of the charging station.

The design of a single EVCS is explained in [6] where the EV demand is modeled as an Erlang B queueing model and includes the implementation of renewable energy sources. The solution to the sizing problem is achieved using genetic algorithms to overcome the problem's complexity.

The focus of our work in this thesis is primarily to model EVCS with queueing models that are derived from Markov chain modeling of EVCS states in continuous time.

2.1.2 Considering the User's Perspective

Range anxiety, the fear of running out of battery charge and being stranded, is a significant concern for EV owners and can affect the location and utilization of charging stations. Therefore, studies have been conducted to identify optimal locations for EVCSs to alleviate range anxiety and maximize user convenience. Charging service providers must invest in building more charging stations to alleviate this significant concern and satisfy EV owners that they will not be stranded with a dead EV battery [22]. Urban congested areas will likely adopt fast-charging equipment. While it could result in efficient drive-throughs, it may also cause a substantial surge in electricity peak demand.

The mobility of EVs plays a key role in the expansion of electrified transportation systems in urban areas. To tackle the long total trip time of EVs in this system and thus improve users satisfaction, authors in reference [23] model the routing problem as a multi-server queueing system where the single and multiple charger units are modeled with $M/M/1$ and $M/M/c$ queues, respectively. The stochastic convex optimization is then solved using the Lagrangian method.

We consider blocking probability as one of the major factors driving the sizing decision for EVCS and hence we deploy blocking probability in our problem description in Chapter 4.

2.1.3 Installation and Service Cost Optimization

When designing and operating EVCSs, it is important to consider investment and service costs. Several studies have explored cost-effective charging station configurations and operating strategies to minimize capital and operational expenses while ensuring optimal performance. Most EV owners can charge their vehicles overnight using level 1 or 2 charging equipment at home. However, for about 40% of Americans who lack access to private charging, access to multi-

unit dwellings, workplaces, or public charging facilities is necessary, highlighting the need for commercial-scale charging stations that can accommodate multiple EVs. Nevertheless, the main challenge is managing the significant impact of EVCS penetration on the main grid. Capacity sizing and siting of electric vehicle charging stations have been extensively researched in the literature.

Authors in reference [24] introduce a simulation-based approach to generate trip trajectories and simulate charging behavior based on various trip attributes. This simulation tool is an input to the optimization problem that considers the total system cost, including charging stations and charger installation costs, charging, queueing, and detouring delays. The objective function implemented in [24] includes the total delay cost experienced by EV users assuming that there is an infinite capacity for waiting in the queue.

A scheduling problem is investigated for multiple EVCSs where they receive EV charging requests and the goal is that each EVCS aims to maximize the amount of charged energy and the number of charged EVs [25]. The authors propose an agent-based simulation approach, where the EVs announce their requests to the stations and each station computes an optimal solution using ILP techniques.

In our study, we determine the optimal sizing of a single EVCS where the assumption is that the maximum number of charger pods is restricted. Rather than accounting for delay costs, we focus on the expenses incurred due to the blocking rate. To address the optimization problem, we utilize a decomposition technique for smaller-scale issues, and we intend to explore heuristic methods for larger-scale networks in future research.

2.1.4   Sizing of EVCS and Power Network Expansion

Location and expansion planning are crucial considerations for the effective deployment and operation of EVCSs. The scientific literature has investigated multiple approaches to identify the optimal number, location, and type

10

of charging stations required to meet the surging demand for EV charging services. Additionally, transformer capacity limitations imposed by the grid can restrict the installation of EVCSs in some areas. Innovative solutions such as load management techniques have been studied to address these limitations and facilitate the smooth operation of EVCSs. Reference [26] is among the early works on siting and sizing of EVCS. The paper proposes a two-stage optimization approach, whereby the optimal locations of EVCSs are determined in the first stage, and the optimal sizing is then incorporated to minimize the total costs associated with EVCS planning. To solve this problem, the authors have formulated a modified primal-dual interior point algorithm. A multi-objective EVCS planning problem is introduced in [27] where the charging service allocation is achieved ensuring that power loss and voltage deviations are minimized. The data-envelopment analysis (DEA) is a multidimensional measurement method incorporating multiple input and output variables that is a data-oriented method for the final decision-making. The authors used DEA to find the optimal solution and the planning problem is solved using the cross-entropy method. DCFCs are desirable choices for EV owners when considering the charging session duration. However, the investment cost and high operation impact of these EVCS types on the main grid is still a big challenge. Reference [28] elaborates on the integration problem of a network of fast charging stations into the power grid from both the power grid and user satisfaction perspectives. The authors address the strain of high penetration of EVs at fast DC EVCS on the power grid and tackle this issue along with reducing the blocking probability at EVCS. The relationship between the size of an EVCS with DC fast chargers and customer satisfaction is investigated in [10] where statistical approaches, including Monte Carlo simulation, are used to estimate the charging impact of EVCS and service quality, and an optimization problem is solved to determine the number and capacity of ports. In [29] a chance-constrained stochastic model for planning EVCS is presented where a

mixed integer programming model is developed to determine the sizing and siting of EVCS. Foundational work is investigated to find locations of EVCS to maximize their usability by private EV owners where a combination of level 1 and level 2 chargers is preferred over the adoption of only level 2 chargers [30].

In some works, the expansion planning is inspected from the power grid perspective. For instance, in [31], the authors explain a power grid expansion plan to support energy requirements from an uncertain set of EVs geographically dispersed over a region in a two-stage stochastic programming approach. The first stage determines where to expand the power grid. In the second stage, they determine where to locate charging stations and intuitively the locations are selected where ample energy supply can be provided by the power grid. The sizing problem of the transformer for a parking lot with chargers is explained in [32] assuming that information about EV arrivals is known a priori.

Another line of work focuses on optimizing the sizing and siting of EVCS considering the interaction of power and transportation traffic as two integrated networks. BCMP[1] queueing-based modeling of the network of EVCS is investigated in [34] where the traffic flow data is optimally assigned to the transportation network to determine the capacity of charging stations. The proposed sizing candidate is then evaluated based on the grid load deployment capacity.

Reference [32] models a charging station with a $M/M/1$ queueing system connected to a distribution feeder. An algorithm is developed in [8] to exploit the EVCS charging capacity by minimizing the service drop rate. The authors modeled the EVCS as a dual charging mode queueing system with multiple servers.

Fast charging stations will soon be installed on highways to rapidly recharge the batteries. An origin-destination analysis is performed in [35] to obtain potential locations for EVs to charge and the capacity of each station is identified

---

[1]A BCMP network is a class of queueing networks for which a product-form equilibrium distribution exists. It is a significant extension to a Jackson network [33].

using a queueing model.

Another work that explains the coordination of distributed generation, EVCS, and battery storage is reference [36]. In this paper, the authors focus on the system life cycle cost by maximizing the grid power usage.

Another recent work that explores siting and sizing of EVCS considers the finite queue length at EVCS in $M/M/k/N$ systems [37]. The objective of the optimization problem (akin to prior works) is to minimize the total EVCS costs.

Capacity provisioning is studied in the problem of electric taxi transportation where EVs have limited dwelling times at EVCS locations which are modeled as $M/M/k/N$ queue [38]. The objective is to minimize the infrastructure investment. The authors simplify the models with regression and logarithmic transformation and solve the optimization problem using integer linear programming.

2.2 Sizing of EVCS Jointly with Solar Panel and Battery Storage Systems

The sizing of EVCSs is a critical consideration when designing charging infrastructure. Incorporating solar panels and battery storage systems can help to increase the efficiency of charging stations and reduce their environmental impact. Many efforts are put into sizing PV and BESS jointly in smart houses [39] and microgrids [40, 41]. The joint operation of EVCS, PV, and BESS leads to mitigating the need for the grid power and meeting the charging load or compensating the total amount of power that must be bought from the grid [42]. A multidisciplinary approach to jointly plan PEV charging stations and distributed PV systems in a coupled transportation and power network is introduced in [43]. They formulate a two-stage stochastic programming model to determine the locations and sizes of 1) PEV charging stations and 2) PV power plants.

A two-stage optimization problem is proposed in [9] to solve the siting of EVCS along with the solar panel and battery storage schedule. The authors minimize the energy consumption of EVs with respect to traffic congestion. The capacity allocation problem is solved using heuristic algorithms.

A queueing network model of EVCS supplied with RES is explained in [44] where EVs are modeled as platoons. The uncertainty associated with renewable energy, EV arrival behavior, and charging price variation is considered.

A number of works have studied how to partially or completely rely on renewable energy sources which relieve the burden from the main grid. Authors in [45] present a strategy based on simple search algorithms to find optimal sizing for solar panels and battery energy storage. In more recent works, a robust sizing of RES and BESS for the optimal sizing option of a single charging station is analyzed in [46] where the robust sizing option is selected based on the Chebyshev inequality, allowing the joint sizing of RES and BESS for selected EVCS sizing options.

The algorithm presented in Reference [47] suggests an optimization-based approach for allocating charging stations to PEVs in a commercial area. The primary objective of this approach is to increase the adoption of PV panels and reduce the negative impact of EV loads. A CS sizing algorithm based on queuing theory is proposed in [48]. This algorithm aims to improve the capacity utilization of charging stations while also benefiting EV users.

Quality of service (QoS) requirements and various sizing strategies are investigated in [49] where the operation of smart chargers is also included in the optimization problem. Reference [50] presents a multistage distribution planning model to coordinate the joint operation of RES, BESS, and EVCS.

Feasibility analysis of EVCS equipped with DERs including wind and solar energy is the focus of [51] where a conventional solar energy sizing strategy is taken into account for pure EV, hybrid EV (HEV), plug-in HEV (PHEV), and the solar-powered charging stations.

Sizing of a shared EVCS for a car rental company is investigated in [52] where solar-powered parking lots are considered, and the pick-up/drop-off times of vehicles are known. Based on this assumption, a linear programming problem is solved to maximize the utilization of solar energy while maintaining the same charging level of all EVs.

Chapter 3

Electric Vehicle Charging Station: Optimization of Queueing Networks

The modeling of traffic networks for a population of EVs is based on the queueing theory. Charging ports are equivalent to servers as EVs have to charge up their battery at EVCS. Our goal is to analyze the behavior of EVs at charging stations and model the whole charging station as a queueing system. In this chapter, we review the fundamental results from the queueing theory that assist us in developing the model for an EVCS.

With the burgeoning proliferation of EVs, the imperative of installing additional charging infrastructure and suitably sizing charging stations become increasingly paramount. Given the concomitant high-load impact that these charging stations engender upon the electrical grid, utility operators must effectively harmonize the load distribution amongst charging stations, all the while assiduously adhering to an array of performance metrics (such as blocking probability, average response time, and quality time) to ensure optimal user experience.

Initially, we conduct an examination of the EVCS concept and subsequently

deliberate on the EV workload modeling at charging stations. Through empirical demonstration, we establish that the EV charging demand at charging stations conforms to an exponential distribution, and arrivals at the charging station adhere to the Poisson process, which are the two essential factors in characterizing M/M/... queueing models. Kendall's notation, which denotes the M/M/k/N system of notation, is utilized to identify the distinct attributes of a queuing model. The first two "M"s signify the Markovian or memoryless qualities, while the third letter, "k", represents the number of servers that are actively engaged in the queuing system. In cases where a fourth term "N" is present, it signifies the maximum number of users permitted to join the queuing system, with the "N+1" user being excluded. Finally, we determine the limiting probability for the distinct case of a solitary EVCS modeled as M/M/k/k.

3.1   Definitions

Here we briefly define some of the queueing theory terms that are used in the context of EV charging in this thesis.

Job Size   The amount of energy necessary to satisfy the energy requirements of an EV is postulated as a constant rate of charging, denoting the maximum charge power that the charger is capable of supporting. In the event that an EV necessitates charging for a total of 33 kWh utilizing a charger with an 11 kWh maximum rate, the size of the job is quantified as 3 hours, assuming the unit time is equivalent to 1 hour.

Arrival rate   The number of EVs that arrive at a charging station per unit of time. It is denoted by λ.

Inter-arrival The time between two successive arrivals at the charging station. In Chapter 4, we show that this rate for the ACN dataset [53] follows an exponential distribution in an uncontrolled charging station.

Service average response time The expected amount of time (denoted by $\mathbb{E}[T]$) for an EV that arrives at a charging station until it gets its service (i.e. waiting time in the queue plus the service time).

Waiting time or Delay The time a job waits until its service starts is denoted by $\mathbb{T}[Q]$.

Mean waiting time The expected waiting time when an EV arrives at the queue until its service begins. Generally the mean waiting time of a system is $\mathbb{E}[T_Q] = \mathbb{E}[T] - \mathbb{E}[S]$.

Number of jobs in the system N (population size) Total number of EVs both in the queue line and in service.

Number of jobs in the queue N_Q Only EVs that are waiting for their turn to get service.

Blocking probability is the probability that a user that arrives at the system cannot join the queue. This is available only for queueing systems of type $M/M/k/N$ as will be discussed later in this thesis.

Utilization denoted by ρ_i (for a single server) is the fraction of time that the charger i is busy.

Squared coefficient of variation C_X^2 is the squared coefficient of variation of random variable X defined as $C_X^2 = \frac{Var[X]}{E[X]^2}$. Note that for exponential distributions $C_X^2 = 1$.

3.2 EVCS Workload Modelling

Within the realm of queueing theory, the intricacies of a queue are dictated by a stochastic process, wherein the job service prerequisites, such as the EV charging demand, and the interarrival intervals of jobs, are deemed to be random variables. It is noteworthy that the general stochastic model of a queueing system is not necessarily always amenable to analytical tractability. Nevertheless, as we shall expound in subsequent sections, the Markovian assumptions serve to greatly simplify the analysis. In Section 3.4, we undertake an empirical exploration of diverse EV charging stations and scrutinize real-world data from EV charging stations, thereby ascertaining the plausibility of the Markovian assumption and substantiating its inherent characteristics.

The workload of a charging station is predominantly reliant on the arrival rate of EVs in the system, along with their respective service requisites. Ordinarily, the job size of an incoming EV is not known a priori, and the service rate may not be fixed whilst the jobs are being serviced. Nonetheless, to simplify the problem at hand, we posit that the EVs are charged at the maximum power that is supported by the charger. In light of this, we can model the arrival process utilizing a Poisson distribution with λ serving as the parameter, owing to the independent arrival of EVs at the charging station and the exponential distribution governing their interarrival times.

3.3 Steady State Queuing Analysis

The queueing models that were used in the literature for EVCS modeling are explained here and the derivation of the limiting probability and performance measures (response time, blocking probability, etc.) are explained in detail.

3.3.1 M/M/1 Queues

This model indicates that there is a single charger with EVs arriving at the charger following a Poisson process. The first M indicates that the inter-arrival times are exponentially distributed. The second M characterizes the distribution of service times. The third term is the number of charger ports available to provide service. Based on Kendall's notation, there might be a 4th term and it is by default infinity for M/M/k queues indicating that the capacity of the system (i.e., the sum of the queue length and the user in service) is unbounded.

For this queuing system, we have the following definitions:

The birth and death process for each charger port holds and the balancing equations are expressed as:

$$p_0.\lambda = p_1.\mu \tag{3.1}$$

$$p_1.(\lambda + \mu) = p_0.\lambda + p_2.\mu \tag{3.2}$$

$$...$$

$$\rightarrow \; p_i = (\frac{\lambda}{\mu})^i.p_0 \tag{3.3}$$

where p_i is the probability that there are i users in the queueing system (both in the queue and at service). λ and μ are respectively the arrival and service rates at EVCS.

Considering the sum of all probabilities equates to one, we solve for p_0:

$$\sum_{i=0}^{\infty} p_i = 1 \;\rightarrow\; p_0 = 1 - \frac{\lambda}{\mu} \tag{3.4}$$

the ratio $\dfrac{\lambda}{\mu}$ is called the server utilization (ρ). The condition $\rho < 1$ must be held for a stable queuing system with infinite queue capacity.

Let the number of users in the system (i.e., system length) be denoted as

$\mathbb{E}[N]$. The general term for the number of customers in the system is given by:

$$\mathbb{E}[N] = \sum_{i=0}^{\infty} i.p_i \tag{3.5}$$

$$= \frac{\rho}{1 - \rho} \quad \text{for M/M/1 system} \tag{3.6}$$

The expected length of the queue also referred to as queue occupancy ($\mathbb{E}[Q]$ or L_q or Q) is the expected length of the system $\mathbb{E}[N]$ minus the server effective utilization ρ_{eff}. λ_{eff} is the actual arrival rate seen at the EVCS and ρ_{eff} is derived accordingly.

$$\mathbb{E}[Q] = L_q = \mathbb{E}[N] - \rho_{\text{eff}} = \frac{\rho_{\text{eff}}^2}{1 - \rho_{\text{eff}}} \tag{3.7}$$

$$\rho_{\text{eff}} = \frac{\lambda_{\text{eff}}}{\mu} \tag{3.8}$$

$$\lambda_{\text{eff}}^{M/M/1} = \lambda^{M/M/1} \tag{3.9}$$

From Little's law, the average time in the system or total delay is determined as:

$$\mathbb{E}[T] = D = \frac{\mathbb{E}[N]}{\lambda_{\text{eff}}} \tag{3.10}$$

$$\mathbb{E}[T]^{M/M/1} = \frac{1}{\mu - \lambda_{\text{eff}}} \tag{3.11}$$

$$\mathbb{E}[T_Q]^{M/M/1} = \mathbb{E}[T]^{M/M/1} - \mathbb{E}[S] \tag{3.12}$$

$$= \frac{1}{\mu - \lambda} - \frac{1}{\mu} = \frac{\rho}{\mu - \lambda} \tag{3.13}$$

3.3.2   M/M/k Queues

M/M/k queues are a type of queueing system in which arrivals are modeled as a Poisson process, and service times are modeled as exponentially distributed. The 'k' in M/M/k refers to the number of service channels or servers available to serve the incoming arrivals.

In an M/M/k queue, there can be up to 'k' parallel service channels available for serving EVs. When an EV arrives, it joins the shortest queue or channel, and upon reaching the front of the queue, it is served by an available server. If all 'k' servers are busy, the arrival joins the queue and waits for the next available server.

The main difference between M/M/k and M/M/1 queues is the number of service channels available. In an M/M/1 queue, there is only one server available to serve the incoming arrivals. When an arrival occurs, it joins the queue and waits for the server to become available. Once the server finishes serving the customer at the front of the queue, it becomes available to serve the next customer.

M/M/k queues are often used in scenarios where multiple servers can provide service to the arrivals.

One important metric in evaluating the performance of M/M/k queues is the probability of the queue being full, or the utilization of the servers. When the arrival rate is higher than the service rate, the queue can become full, and customers may experience longer waiting times or even abandon the queue. Thus, it is essential to design the queueing system to ensure that the servers are utilized efficiently without causing excessive waiting times for customers.

3.3.3   M/M/k/N Queues

Prior to the formulation for the $M/M/k/N$ queuing model, let's elaborate on $M/M/1/N$ where we have a single charger with the cap on the EV population. This would be helpful when designing the optimization problem considering an extension of $M/M/1/N$ to k identical chargers with a shared pool of service rate μ_{max}. for M/M/1/N system, the limiting probabilities explained earlier for $M/M/1$ are valid except that the number of states is finite (until N). It is

expressed as:

$$\Sigma_{i=0}^{N} p_i = 1 \tag{3.14}$$

$$p_0 = \frac{1-\rho}{1-\rho^{N+1}} \tag{3.15}$$

$$p_k = \rho^k [\frac{1-\rho}{1-\rho(N+1)}] \tag{3.16}$$

$$\mathbb{E}[N] = \Sigma_{i=0}^{N} i\rho^i = \frac{\rho}{1-\rho}[\frac{1 + N\rho^{N+1} - (N+1)\rho^N}{1-\rho^{N+1}}] \tag{3.17}$$

As can be seen, the mean number of users in the system $\mathbb{E}[N]$ for this case has an extra term. The formulation for this queuing model will be different since there is a cap on the queue length. Hence, the following definitions and terms hold for $M/M/k/N$ queuing systems:

$$\Sigma_{i=0}^{N} p_i = 1 \tag{3.18}$$

$$\lambda_{\text{eff}} = \lambda.(1 - p_N) \tag{3.19}$$

$$\mathbb{E}[T] = \frac{\mathbb{E}[N]}{\lambda_{\text{eff}}} \tag{3.20}$$

3.3.4   Blocking Probability in M/M/k/N Queues

The blocking probability of a queueing system is the probability that a customer is blocked due to a lack of resources. For an M/M/k/N queueing system, where arrivals follow a Poisson distribution with rate λ and service times follow an exponential distribution with rate μ, there are k servers and a maximum capacity of N customers in the system.

The blocking probability, denoted by P_b, is the probability that all k servers are busy and there are already N customers in the system. In this case, any arriving customer will be blocked and unable to access the service.

The blocking probability can be derived by considering the limiting probability of the system being in the blocking state. Using the birth-and-death process, we can calculate the probability of each state from $i = 0$ to $i = k$.

Let P_i be the probability of the system being in state i, where i is the number of customers in the system, including those being served. Then, we have:

$$p_{i+1} = \frac{\lambda}{\mu} p_i, \quad i = 1, 2, ..., k-1 \tag{3.21}$$

where P_0 is the probability of the system being empty and P_k is the probability of the system being in the blocking state.

Using the normalization condition $\sum_{i=0}^{N} P_i = 1$, we can solve for P_0 as:

$$p_0 = \left(\sum_{i=0}^{k} \frac{(\lambda/\mu)^i}{i!} + \frac{(\lambda/\mu)^k}{k!} \sum_{i=k+1}^{N} \frac{(\lambda/\mu)^{i-k}}{k^{i-k}} \right)^{-1} \tag{3.22}$$

and for P_i as:

$$p_i = \begin{cases} \frac{(\lambda/\mu)^i}{i!} p_0 & i = 1, 2, ..., k \\[2ex] \frac{(\lambda/\mu)^i}{k! k^{(i-k)}} p_0 & i = k+1, ..., N \end{cases} \tag{3.23}$$

Therefore, the blocking probability is given by:

$$p_{blk} = p_k \tag{3.24}$$

The Erlang B formula is a special case of the blocking probability formula for a M/M/k queueing system with infinite capacity ($N = \infty$). In this case, the formula simplifies to:

$$p_b = \frac{(\frac{\lambda}{\mu})^k}{k!} \frac{1}{\sum_{i=0}^{k} \frac{(\lambda/\mu)^i}{i!}} \tag{3.25}$$

The Erlang B formula is commonly used in telecommunications to calculate the blocking probability in telephone networks. It assumes that blocked calls are immediately cleared and do not retry, which is a reasonable approximation for busy hour traffic in large networks.

3.4 Modeling the EVCS Workload based on Real Data

Many EVCS operators (both state and privately owned entities) provide their charging session records for public access and research purposes. A comprehensive review of EV open datasets is presented in [54]. However, no work has explored whether standard queueing theory assumptions hold for real datasets.

This section is dedicated to providing performance measures for some EVCS charging stations. This evaluation analysis is significant to recognize the existing EVCS charging model to facilitate the formulation of an optimization problem.

We look at four publicly available datasets:

- The ACN dataset provides a record of EV arrivals and the charge demand at Caltech Pasadena parking station and JPL parking lots [53].

- The Boulder-Colorado city provides the charging records of 20 charging stations [55] where all installed chargers are level-2 (with max charge power of 11 kW).

- ElaadNL is an innovation center based in the Netherlands that manages smart charging strategies nationwide. They provide open data for thousands of charging sessions that occurred in their charging infrastructure [56].

Common data features among the aforementioned datasets are

- arrival time

- charging duration

- departure time

- amount of charge delivered
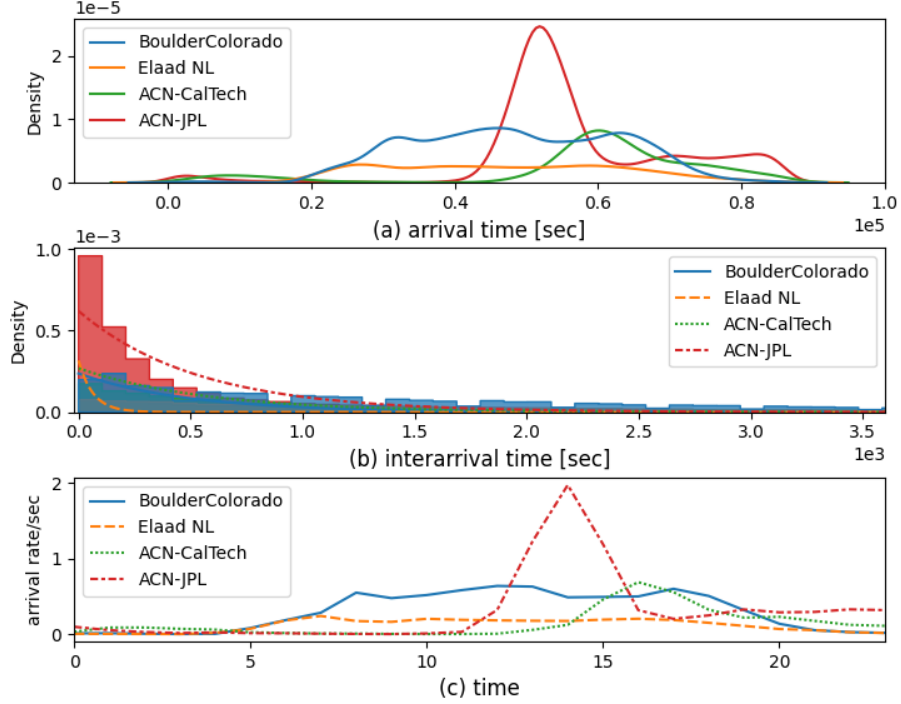
Figure 3.1: Arrival rate and inter-arrival time distributions. The dotted lines in (b) represent the best-fitted exponential distribution.

These parameters are useful in determining the performance measures of a queueing-based model.

Our goal is to find the maximum likelihood estimator of the parameters representing the arrival rate and service rate for these datasets. As mentioned earlier, the majority of existing real-world examples of queueing systems are based on a Markov process which significantly simplifies the analysis. However, if the service distribution in any queueing system does not have the memoryless property (i.e. it is not an exponential distribution) then the analysis of that system becomes complex and it is outside the scope of this research work.

Fig. 3.1, illustrates the distribution of arrivals extracted from four datasets. The exact time of arrivals is shown in Fig. 3.1(a) where the precision of arrivals is presented in seconds. The inter-arrival time of two consecutive EVs (shown
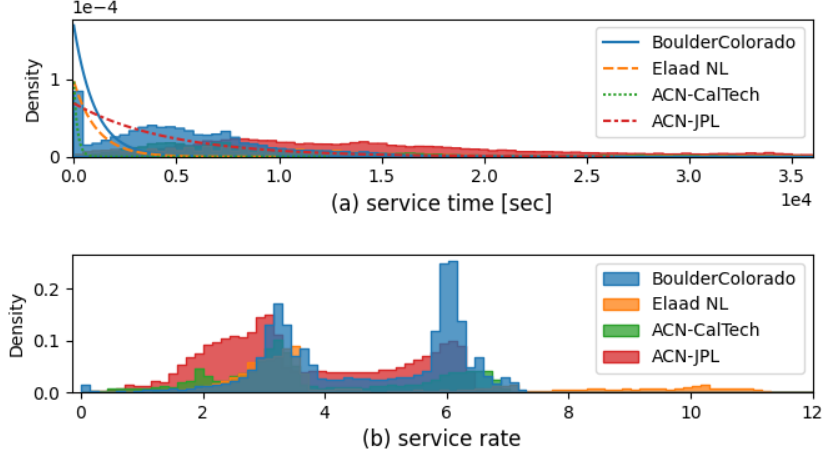
Figure 3.2: Service time/rate and requirement of four datasets. The dotted lines in (a) represent the MLE exponential distribution

in Fig. 3.1(b)) is determined using the following formulation

$$S_{i+1} = A_{i+1} - A_i \qquad (3.26)$$

where S_{i+1} is the inter arrival time between two EV arrivals A_{i+1} and A_i at times $i+1$ and i, respectively. An exponential distribution using the maximum likelihood estimation (MLE) method is fitted to the inter-arrival times. The inverse of inter-arrival time gives us the arrival rate and the estimated value denoted by $\tilde{\lambda}$ is shown in Table 3.1.

Fig. 3.1(c) shows the arrival rate (per second) of EVs to the charging station in the four datasets. For instance, the arrival rate for the ACN dataset has a peak value of around 2 pm.

Fig. 3.2(a) shows the service time and service requirement distribution of four data sets.

The same approach is taken to fit an exponential distribution to the service time, depicted by the dashed lines in Fig. 3.2(a) and the estimated service rates denoted by $\tilde{\mu}$. Their values are presented in Table 3.1. The estimated values follow closely to the actual service rate values which proves that Markovian

Table 3.1: Queueing Parameters Estimated in each Dataset

	Boulder Colorado	Elaad NL	ACN-CalTech	ACN-JPL
C_μ^2	16.23	1.48	0.77	0.21
$\tilde{\mu}$	0.61	0.35	0.35	0.25
$\tilde{\lambda}$	0.85	1.14	0.97	2.24

modeling is a suitable option for charging stations. We use the resulting values from Table 3.1 for the ACN dataset in an optimization problem presented in Chapter 4 of the thesis.

Chapter 4

Capacity Provisioning for a Charging Station Equipped with PV System

EVs powered by renewable electricity can reduce petroleum usage and greenhouse emissions [57]. From the grid's perspective, the high impact of charging EVs at charging stations is the main concern of utility providers. One solution is to install onsite renewable technologies such as PV solar panels and battery storage systems to curtail the sharp EV loads.

In this chapter, our goal is to formulate a two-level optimization problem to find the smallest number of chargers installed at a charging station to meet EV users' satisfaction. The designated EVCS is equipped with two different charging levels because it improves the charging efficiency of the station as concluded in [30]. This is translated into a performance measure for a queueing system represented by $M/M/k/k$. Then using the resulting number of charger ports, PV panel, and battery storage capacity are optimized to minimize energy dependency on the electricity grid. In our work, we attempt to provide practical, robust advice on system sizing to ensure that it is resistant to perturbations to the inputs (i.e. charging patterns).

In summary, the contributions of this chapter are as follows:

- Queueing model of EVCS considering two levels of chargers is developed

- We determine the blocking probability of EVCS is determined

- We solve an optimization problem for the number of chargers to meet a minimum blocking probability

- Having the sizing of EVCS, we solve a MILP optimization problem to find the minimum PV and battery capacity

- We find a robust size of PV and battery to minimize the dependency on the main grid

4.1   EVCS Queueing Model

We use a Markovian model to characterize the EVCS demand and find the blocking probability. A reasonable choice of the state space is the number of EVs being served at the station [58]. Some prior works assume that EV owners communicate with the charging service provider so the charging demand is known ahead of time [59]. This approach is not practical and one solution to this is to use the historical data to predict the distribution of service requirements similar to what has been done in computer networks [60]. By analyzing the actual data in section 4.3, we show that the Poisson process is an accurate model for EV arrival and that the exponential distribution is a good fit for EV charge requirements. We model a single EVCS as an $M/M/k/k$ queue equipped with two types of servers (fast and slow) and determine the blocking probability by finding the steady state distribution of the Markov chain shown in Fig. 4.1. This birth-death process has $k = n_{L_3} + n_{L_2}$ states. The arrival rate is denoted by λ. We divide the charge requirement of each EV by the charge rate of the respective charger to get the service time distribution of L_2 and L_3
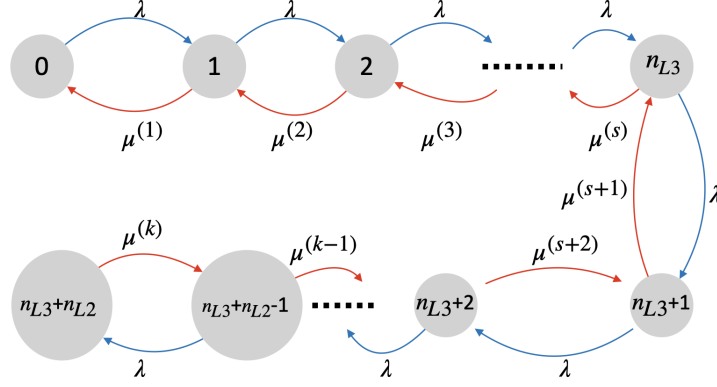
Figure 4.1: State transition diagram for the proposed CTMC of EVCS constructed with n_{L_2} and n_{L_3} number of L_2 and L_3 chargers, respectively.

chargers. The mean of these exponential distributions is denoted by $1/\mu_2$ and $1/\mu_3$, respectively. The service completion rate in state s, denoted by $\mu^{(s)}$, can be written as:

$$\mu^{(s)} = \begin{cases} s\mu_3 & 0 \leq s \leq n_{L3}, \\ n_{L3}\mu_3 + (s - n_{L3})\mu_2 & n_{L3} < s \leq k. \end{cases} \tag{4.1}$$

To calculate the total amount of real power consumed by the EVCS in a state, we associate every state s with the total power delivered to EVs by the active chargers:

$$P_L(s) = \begin{cases} \frac{s \cdot \overline{P}_{L3}}{\eta_3} & 0 \leq s \leq n_{L3}, \\ \frac{n_{L3} \cdot \overline{P}_{L3}}{\eta_3} + \frac{(s - n_{L3}) \cdot \overline{P}_{L2}}{\eta_2} & n_{L3} < s \leq k, \end{cases} \tag{4.2}$$

where η_2 and η_3 are the charging efficiency of L_2 and L_3 chargers, respectively.

We determine λ by calculating the average number of EV arrivals per unit of time. We find the best distribution fit for the inter arrivals and we show that the error of the best fit exponential distribution and the actual recorded values is less than 5% (see Fig. 4.2). μ_2 and μ_3 are determined by calculating the amount of time required to charge each EV based on their charging requirement (which is also accessible in recorded history). The service time requirement is the ratio of each EV charge requirement (in kWh) to the maximum power rate

of chargers denoted by $\overline{P}_2$ and $\overline{P}_3$ for L_2 and L_3, respectively.

Since Poisson arrivals see time averages (a.k.a. the PASTA property), the probability that an EV finds no available charger upon arrival is the stationary probability of being in state $k = n_{L_3} + n_{L_2}$. It can be written as:

$$\pi_{blk} = \frac{\lambda^{(n_{L_3}+n_{L_2})}}{n_{L_3}! \, \mu_3^{n_{L_3}} \prod_{i=1}^{n_{L_2}} (n_{L_3}\mu_3 + i\mu_2)} \pi(0), \tag{4.3}$$

where $\pi(0)$ is the stationary probability that the EVCS is empty and can be calculated from the normalizing equation that states the stationary probabilities must sum to 1:

$$\frac{1}{\pi(0)} = \sum_{i=0}^{n_{L_3}-1} \frac{\lambda^i}{i! \, \mu_3^i} + \sum_{i=n_{L_3}}^{k} \frac{\lambda^i}{n_{L_3}! \, \mu_3^{n_{L_3}} \prod_{j=1}^{i-n_{L_3}} (n_{L_3}\mu_3 + j\mu_2)}$$

The full derivation of limiting probabilities is explained in the appendix A. Assuming that we have access to representative traffic data and historical charging demand data, for example, from [53], we can estimate the arrival and service rates. The resulting transition rate matrix can be used to generate sample paths of a desired length. We can then calculate the net demand of the EVCS for each sample path. The PV generation traces are based on publicly available solar radiation data collected at regular intervals (e.g., hourly) for the specific location of the EVCS from the Solcast API[1] and fed to PVWatts[2]. It is worth noting that the EV charging and PV generation datasets must have the same temporal resolution, otherwise we have to use a re-sampling technique. Once both traces are ready, they can be sampled from to create *scenarios* for the optimization problems defined in the next section.

---

[1] https://solcast.com/solar-data-api/api/
[2] https://pvwatts.nrel.gov/pvwatts.php

4.2   Joint Sizing of EVCS and Co-located DER

We start with solving the first problem which deals with finding all feasible numbers of level 3 and level 2 chargers representing as (n_{L_3}, n_{L_2}) pairs. In the next step, given a feasible EVCS design and a fixed BESS size, we find the minimum size of the PV system such that the ratio of unmet load (RUL) by DER to total load is less than a threshold δ.

To find all possible sizing options for the EVCS, we solve the following feasibility problem

$$\min_{n_{L_3}, n_{L_2}} \quad Z \tag{4.4a}$$

$$s.t. \quad \pi_{blk} \leq \theta, \tag{4.4b}$$

$$\frac{n_{L_3}\overline{P}_{L_3}}{\eta_3} + \frac{n_{L_2}\overline{P}_{L_2}}{\eta_2} \leq \overline{P}_G, \tag{4.4c}$$

where Z is an arbitrary constant, and $\overline{P}_G$ is a limit imposed by the power utility based on the rating of the transformer that feeds the EVCS. Constraint (4.4b) is the performance measure hard constraint and gives the lower bound on the required number of L_2 and L_3 chargers (θ is the maximum acceptable blocking probability), while (4.4c) caps the number of chargers with respect to the maximum charging consumption at the station ($\overline{P}_G$). This is a convex problem if we pre-calculate and cache the blocking probability for different (n_{L_3}, n_{L_2}) pairs. Solving (4.4) gives a set $\mathcal{H}$ that includes all tuples $(n_{L_3}^*, n_{L_2}^*)$ that meet the performance measure requirement and do not strain the power grid.

To size the co-located DERs, given a feasible EVCS sizing option ($\in \mathcal{H}$), we solve an optimization problem over T timesteps of equal length, T_u. We denote the power supplied to EVCS directly from PV panels in timestep i by P_{in}^i and the SOC of the BESS by e_b^i. The battery charge (resp. discharge) rate, labeled P_c (resp. P_d), must be less than the BESS power capacity, which is assumed to be a multiple of the battery energy capacity ($\alpha_c E_B$ and $\alpha_d E_B$)

because BESS has a modular structure. P_{cs}^i is the charging station demand at time i, and S^i is the solar energy produced at time i. Given P_{cs}^i and S^i, we solve the following optimization problem to minimize the capacity of the PV system such that DER's RUL is lower than a threshold δ.

$$\min_{C_{pv},P_c,P_d,P_{in},u,e_b} \quad C_{pv} \tag{4.5a}$$

$$s.t. \quad P_c^i + P_{in}^i \leq S^i C_{pv} \tag{4.5b}$$

$$P_{in}^i + P_d^i = P_{cs}^i - e^i \tag{4.5c}$$

$$e_b^0 = E_B \tag{4.5d}$$

$$e_b^{i+1} = e_b^i + P_c^i \eta_c T_u - P_d^i \eta_d T_u \tag{4.5e}$$

$$a_1 P_d^i + b_1 E_B \leq e_b^i \leq a_2 P_c^i + b_2 E_B \tag{4.5f}$$

$$0 \leq P_c^i \leq \alpha_c E_B u^i \tag{4.5g}$$

$$0 \leq P_d^i \leq \alpha_d E_B (1 - u^i) \tag{4.5h}$$

$$E_B, C_{pv}, P_{in}^i, e^i, e_b^i \geq 0 \quad \forall i \tag{4.5i}$$

$$u^i \in \{0,1\} \quad \forall i \tag{4.5j}$$

$$\sum_{i=1}^T e^i \leq \delta \sum_{i=1}^T P_{cs}^i \tag{4.5k}$$

The above problem is a (mixed integer linear programming) MILP and the only integer variable is u. Constraint (4.5b) ensures that the total PV power delivered is less than the PV system output; (4.5c) is the power balance equation that ensures grid power is used to supply the unmet charging demand denoted by e^i; (4.5d)-(4.5h) are related to the battery characteristics and the model is extracted from [61]. (4.5d) is the initial energy state of the battery, (4.5e) represents the state of the energy at each time i, (4.5f) ensures that the battery should not be charged beyond its capacity and the charge power available at the terminal, (4.5g) and (4.5h) are the constraints associated with the charging and discharging instances of the battery, respectively. (4.5k) limits the ratio of

the charging demand that must be supplied from grid power in T time steps to the total charging demand. We solve this optimization problem over intervals of length T that are randomly sampled from the entire dataset. Each sample gives a sizing scenario. We solve the optimization problem for n scenarios, each time setting the BESS capacity to a fixed value.

4.2.1   Robust Sizing Strategy

Solving the two optimization problems introduced earlier in this section for each scenario yields a set $\mathcal{C}$ that contains PV system sizes for a fixed BESS capacity $E_B = B$ and an EVCS sizing option. The cardinality of this set is $N_{pv} \leq n$. Considering the elements of this set, we compute the empirical estimates of the mean $m_{C,N_{pv}}$ and standard deviation $\sigma_{C,N_{pv}}$, and write the Chebyshev inequality [62] as follows:

$$\mathbf{P}\{|C_{pv} - m_{C_{N_{pv}}}| \geq \beta \sigma_{C_{N_{pv}}}\} \leq \min(1, f(\beta)), \tag{4.6}$$

$$f(\beta) = (N_{pv} + 1)^{-1} \left\lfloor \frac{(N_{pv} + 1)(N_{pv}^2 - 1 + N_{pv}\beta^2)}{N_{pv}^2\beta^2} \right\rfloor \tag{4.7}$$

Essentially, Chebyshev's inequality is investigated when the population average and variance are estimated from a sample. The necessary modification to the inequality is simple and is actually valid when (a) the population moments do not exist and (b) the sample is exchangeably distributed. The latter case would include, for example, a sample taken without replacement from a finite population and the independent and identically distributed case [62]. Equation (4.6) gives an upper bound on the probability that the difference between a value of C_{pv} (for any, possibly unseen, scenario) obtained for a BESS of size B and the estimated mean $m_{C_{N_{pv}}}$ exceeds a factor β of the estimated standard deviation $\sigma_{C_{N_{pv}}}$. Note that β is the smallest number that satisfies $f(\beta) \leq \gamma$

and γ is our confidence measure.

$$\min_{\beta} f(\beta) \leq \gamma \tag{4.8}$$

As γ approaches 1, the value of β that satisfies the confidence measure becomes larger. This will result in a more conservative sizing, i.e., the requirement for a larger PV system. In other words, we tend to use more DER capacity to be less dependent on the main grid. Given the value of β, we derive the optimal PV sizing from (4.6), that is $C_{pv}^* = m_{C_{N_{pv}}} + \beta\sigma_{C_{N_{pv}}}$. We use Chebyshev inequality to find an upper estimate for C_{pv}^*. For each value of E_B drawn from an admissible battery capacity range, we construct a set of tuple points (E_B, C_{pv}) comprising several curves along the intersection of $E_B = E_{B'}$ for n samples. Not all sizing curves have values at all E_B selected in the admissible range. (4.6) gives a bound on the probability that the distance between some future value of C_{pv} for a specific $E_{B'}$ from the estimated $m_{C_{pv}}$ exceeds a factor of β. The resulting points can be interpolated to define a curve which can be called Chebyshev curve on C_{pv}, since each point on the curve is a Chebyshev bound on C_{pv} values. Similarly, we construct a Chebyshev curve on E_B for each value of c_{pv} chosen from an admissible range on the solar capacity $C_{pv'}$.

The upper envelope of these Chebyshev curves represents robust system sizes with respect to both E_B and C_{pv} with confidence measure $1 - \gamma$. We use both curves (from PV and BESS sizing) to calculate an upper envelope for DER sizing. We then employ a simple grid search to find the least expensive sizing tuple for C_{pv} and E_B among the points that lie on the upper envelope of the Chebyshev curves.

4.3 Results

The proposed robust sizing methodology is evaluated using real data traces of PV generation from NREL's PVWatts and historical EV charging data from

Table 4.1: Average Arrival and Service Rate Parameters

Year	2018	2019	2020	2021
λ	0.66	0.516	0.68	1.67
μ_2	0.75	0.98	1.17	1.41
μ_3	3.42	4.44	5.31	6.41

the adaptive charging network (ACN) [53] that contains more than 30,000 charging sessions since 2018. We collect the traces for a period of 4 years with hourly resolution. In the next step, we verify that the inter-arrival times and energy requirements follow exponential distributions (see Fig. 4.2), and then estimate the parameter of each distribution to obtain the average arrival and service rates. These rates are used to construct the transition rate matrix and subsequently compute the blocking probability of the CTMC. To account for the future increase in EV penetration, we can multiply the birth rate of the CTMC found empirically by a factor that represents the annual growth in the EV population. The best-fit exponential distributions for the empirical distributions of these two variables result in the Wasserstein distance of 1.09 and 1.40, respectively which verifies the accuracy of our best-fitted distributions. By definition, the average arrival rate λ is the reciprocal of the average inter-arrival time. and hence we can traverse arrival rates from actual data. Similarly, the energy requirement is also exponentially distributed with high accuracy and therefore the EVCS system is modeled with queueing of type M/M/k/k.

Estimated arrival and service time rates are provided for each year in Table 4.1. The arrival rate during the year 2019 is lower because the Caltech EVCS service provider introduced a paid parking. The time step is set to $T_u = 1$ hr (the temporal resolution of the solar irradiance data). The total length of EV charging (P_{cs}) and PV generation (S) traces are $4 \times 365 \times 24 = 35040$ hours. From the traces, we randomly select 100 scenarios, 720 hours each, solve the optimization in (4.5) problem for each scenario, and find the upper envelope of the empirical Chebychev sizing curves. For each scenario, we find the optimal C_{pv} for 30 values of E_B in the set $\mathcal{E}_\mathcal{B} = [45, 700]$. The battery parameters
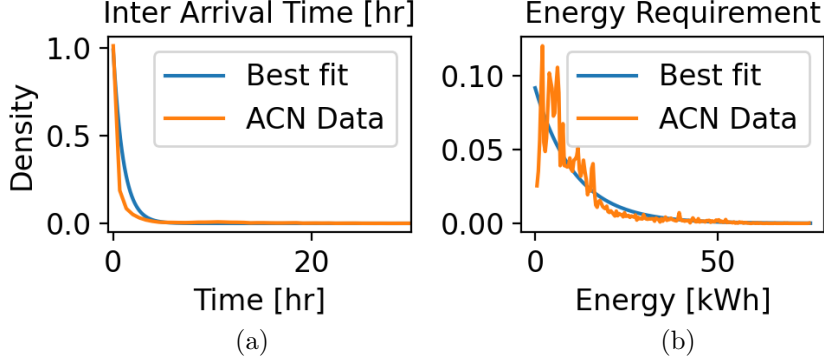
Figure 4.2: Probability density function of (a) the time between two successive arrivals to the EVCS and (b) energy requirement of EVs upon arrival. The best fit is an exponential distribution. $\lambda = 0.98, \mu_2 = 0.98, \mu_3 = 4.44 \ hr^{-1}$.

Table 4.2: Battery Storage and Charging Station Parameters

	Battery Parameters			
Parameter	η_c, η_d	a_1, b_1	a_2, b_2	α_c, α_d
Value	0.99, 1.11	0.053, 0	-0.125, 1	1, 1
	Charging Station Parameters			
Parameter	$\overline{P}_{L2}, \overline{P}_{L3}$	η_2, η_3	δ	γ
Value	11, 50	0.96, 0.98	0.05	0.95

are borrowed from the lithium-ion battery model used in [61]: $\eta_c = -0.99$, $\eta_d = 1.11$, $a_1 = 0.053$, $a_2 = -0.125$, $b_1 = 0$, $b_2 = 1$, $\alpha_c = \alpha_d = 1$. The initial SOC for BESS is set to $e_b^0 = B$. The charging station parameters and other parameters used for the simulations are $\overline{P}_{L_2} = 11$ kW, $\overline{P}_{L_3} = 50$ kW, $\eta_2 = 0.96$, $\eta_3 = 0.98$, $\delta = 0.05$, $\gamma = 0.95$. We use the operating policy to charge/discharge the BESS when PV generation exceeds/fails the load.

4.3.1 EVCS Sizing

The total power consumed by the installed chargers cannot exceed the rated capacity of the transformer, which is assumed to be 250 kW. By solving the feasibility problem (4.4), we found 49 feasible tuples (n_{L_3}, n_{L_2}). The installed costs of L_2 and L_3 chargers are set to \$800 and \$16,500, respectively [32]. Due to the high computation overhead of the optimization, we only investigate two extreme sizing tuples: $\mathcal{T}1$) the least expensive option $(0, 8)$, and $\mathcal{T}2$) the most
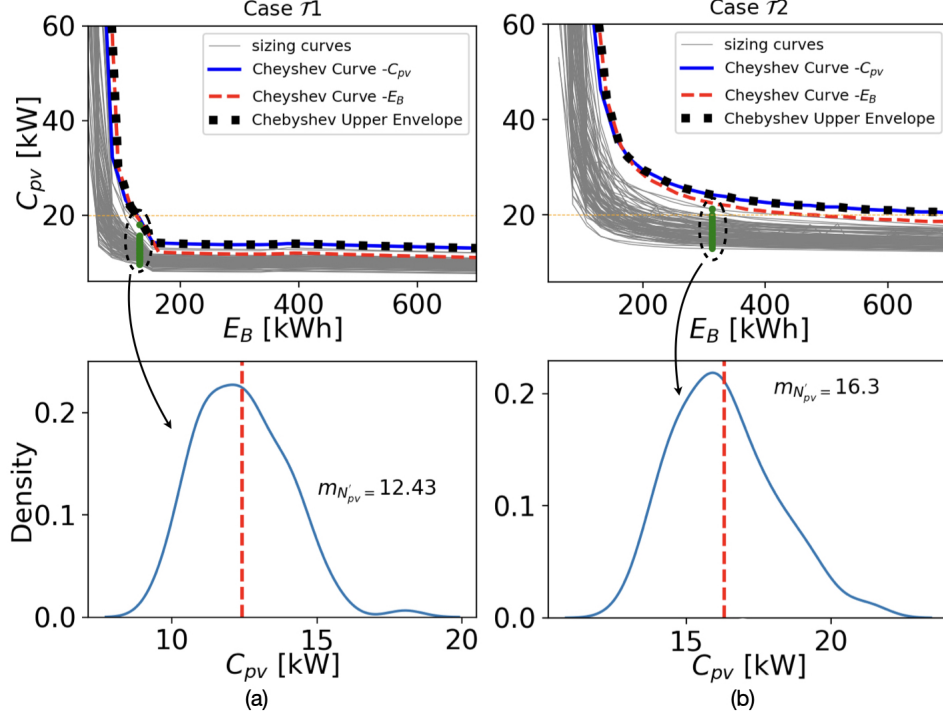
Figure 4.3: Chebyshev bound curves for optimal sizing of C_{pv} for (a) $\mathcal{T}1$ and (b) $\mathcal{T}2$ sizing options with $\delta = 0.05$. Plots in the second row show the empirical distribution of C_{pv} for $E_B = 295kWh$.

expensive option $(4,4)$. Each sizing tuple accounts for a blocking probability of $\pi_{blk,\mathcal{T}1}$=8.8e-8 and $\pi_{blk,\mathcal{T}2}$=2.87e-12 and Both sizing options have very low blocking probability given the current traffic flow rates. Both options yield a blocking probability that is below $\theta = 10^{-6}$.

4.3.2 Solar and Storage Sizing

For each EVCS size, we size the PV system and BESS based on the mean and standard deviation of sizing curves obtained for a sample population of sizing scenarios. Specifically, for each value of E_B, we have 100 curves in the (E_B, C_{pv}) space. Similarly, for each value of C_{pv}, we have 100 curves in the (E_B, C_{pv}) space. We depict the optimal sizing curves and empirical Chebyshev bounds for two specific EVCS sizing options $\mathcal{T}1$ and $\mathcal{T}2$ in Fig. 4.3 for $\delta = 0.05$.
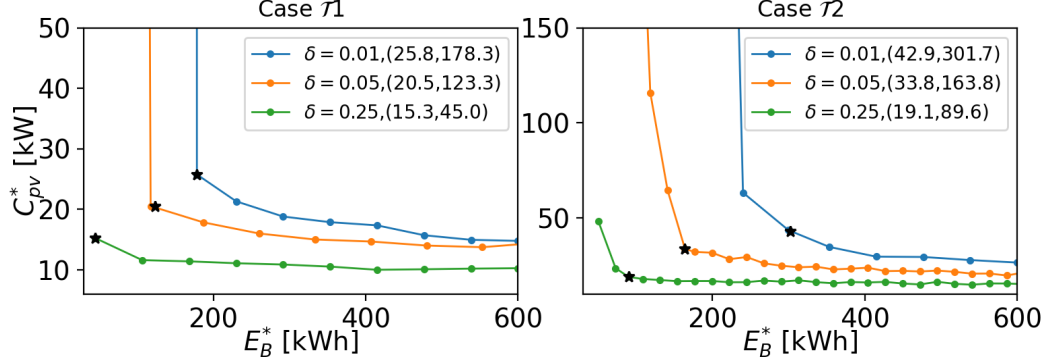
Figure 4.4: Optimal robust sizing recommendation values of δ. In each case, the design with the lowest cost is suggested as (C_{pv}^*, E_B^*) in the legend.

The recommended C_{pv} sizing, as shown in Fig. 4.3 for a randomly selected E_B value, is higher for $\mathcal{T}2$ than $\mathcal{T}1$. This shows that the EVCS equipped with 4 L_2 chargers and 4 L_3 chargers requires approximately 60% higher PV capacity than (0,8). The upper envelope of Chebyshev curves (shown as a dotted black curve in Fig. 4.3) shows our robust sizing recommendation. Considering all (E_B, C_{pv}) points that lie on the upper envelope of Chebyshev curves, we find the least expensive sizing option (C_{pv}^*, E_B^*) assuming the installed cost of \$2,500/kW for PV and \$460/kWh for BESS.

Sensitivity to δ: We evaluate the proposed sizing method for PV and BESS by incorporating different values of δ in (4.5). We illustrate the sizing results for three sample values of δ in Fig 4.4. It can be readily seen that the minimum BESS size increases as the minimum PV system decreases and vice versa. For small values of δ, both PV system and BESS must be considerably larger to satisfy the RUL requirement for a fixed EVCS sizing. The BESS size is especially important for small δ values because it is impossible to meet the RUL requirement before sunrise or after sunset regardless of the PV system size.

Sizing PV-powered EVCS without BESS: We also investigate the case where BESS is not installed in the EVCS to shift PV generation. To solve the sizing problem in this case, we modify the optimization problem in (4.5) by removing
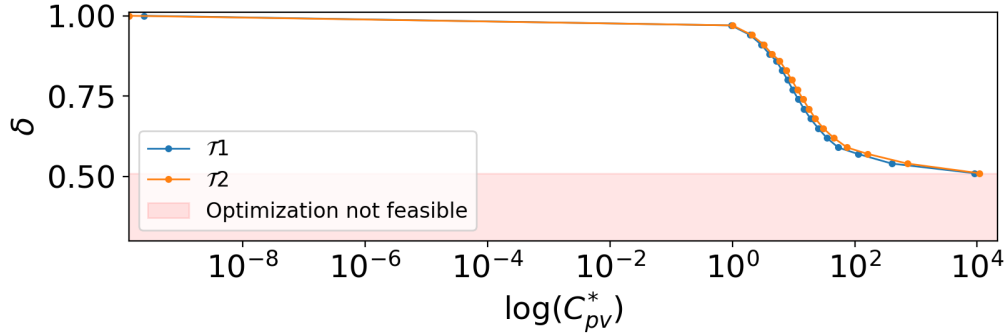
Figure 4.5: Robust sizing of a PV-powered EVCS without BESS.

the constraints and variables corresponding to BESS. The updated optimization problem is a linear program that can be solved efficiently. We find that the sizing problem has no feasible solution for $\delta \leq 0.46$, which is expected because without BESS it is impossible to meet the EVCS demand using PV generation without relying too much on grid power. Fig. 4.5 shows the minimum C_{pv}^* required to meet the grid import requirement for values of $\delta > 0.46$. One interesting observation is that a 10 MW PV system is required to meet the EVCS demand for a threshold of $\delta = 0.51$. Should we install a small 45 kWh BESS, the PV system size could be reduced to 15.25 kW for $\delta = 0.05$ which is 10 times lower than the previous delta value. This underscores the importance of installing a BESS for shifting PV generation.

4.4   Summary

With the falling costs of solar PV and battery technologies, it is anticipated that more EV charging stations will be equipped with DER. In this chapter, we proposed an optimal sizing methodology for an EVCS with two types of chargers and co-located DERs, given the constraints imposed by the power grid operator and customers. Our approach guarantees the robustness of the resulting system size to non-stationarity of PV generation and EV traffic. Using real data, we provide robust sizing recommendations with minimum cost.

Chapter 5

Sizing Multiple Charging Stations

In the previous chapter, we scrutinized the process of sizing a lone charging station with an optimal number of L_2 and L_3 chargers. Nevertheless, the framework we established, albeit practical for an EVCS provider with a solitary charging station, is inadequate to estimate the scale of a network of charging stations disseminated throughout a geographic area. Consequently, an alternative optimization problem is constructed for a network of charging stations dispersed throughout a transportation system, reflecting a realistic business scenario where the service provider possesses a multitude of chargers spread out within a municipality, and their objective is to minimize installation and service expenses.

One of the crucial components of transportation electrification is the infrastructure of charging stations, which is not only confined to residential or private locations but also encompasses workplaces, shopping centers, and street parking stalls [63]. To curtail the charging duration of EVs at public charging stations, DCFC technology coupled with off-board chargers is typically employed. The DCFCs effectively replenish the battery up to 50% of its capacity within 10 to 15 minutes, with a charging power of no less than 30 kW [64].

In the case of multiple charging stations coexisting within a small traffic system, a network model of charging stations is indispensable [17]. Based on this network model, a multiclass capacity planning framework is introduced in [65], and QoS metrics are formulated for the traffic flow of various types of multiclass EV vehicles.

The current chapter pertains to the integration of optimization formulations for the purpose of sizing a network of charging stations. The proposed approach entails modeling traffic as an infinite queue to factor in the commutes[1]. Moreover, the transformer that feeds each EVCS station has a restricted capacity. Other assumptions that are taken into account include:

- EVCS with single port chargers are distributed in a region and each charger port is modeled as an $M/M/1$ queue.

- Traffic flow is modeled as $M/M/\infty$ where the inverse service rate is the time it takes an EV to reach its origin/destination to start another charging session.

- There exists a finite EV population in the network denoted by M_{ev}.

- External arrivals to the network are neglected (i.e. it is a closed queueing network).

5.1   Modeling Traffic Flow and the EVCS Network

EVs that are part of the network arrive at a charging station and upon being serviced, depart from the station. Subsequently, based on the nature of their commute (e.g., grocery shopping, dining out, commuting to or from work),

---

[1]We posit that commutes are independent and identically distributed, with similar random variable distribution being drawn. A similar assumption has been studied in reference [66]

they join the traffic network. The traffic network is presumed to be substantial, facilitating an EV's swift integration into the flow of traffic, thereby initiating their commute without delay. The traffic network is represented as an $M/M/\infty$ where the first M represents that arrival to the queue follows the Poisson process and the second M shows that all commutes are exponentially distributed [67]. A schematic representation of multiple charging station networks and the corresponding queueing network model is shown in Fig. 5.1.

The queueing model that represents an aggregated charging station can be thought of as an $M/M/k$ queueing system (k charger ports at one location) while each particular charger port can be represented as an $M/M/1$ and the two models result in different outcomes [68]. For the purpose of simplification, this research adopts the $M/M/1$ model. However, in actuality, the queue size is finite; nonetheless, to streamline the network modeling process, it is presumed that the queue length is infinite. Each EVCS station is represented as an $M/M/1$ model, with a singular server denoting a solitary charger port. As shown in Fig. 5.1, this is a closed network with a finite number of EVs (M_{ev}). Arrivals at each station are assumed to follow the Poisson process and services are completed following an exponential distribution. The service rate μ_T for the traffic network is small (i.e. it takes each EV a considerable amount of time to finish its commute) compared to the charging rate at EV chargers.

With these assumptions, the multiple EVCS network can be represented as a closed Jackson's Network [69] which has a product-form solution, i.e., limiting probabilities of the whole network is the product of the limiting probabilities of individual queueing systems.

It should be noted that for closed Jackson networks, a normalization factor must be calculated to determine the limiting probabilities [68]. Closed queueing networks represent many practical applications, including flexible manufacturing systems, biotech manufacturing systems etc. [33].

(a)

(b)
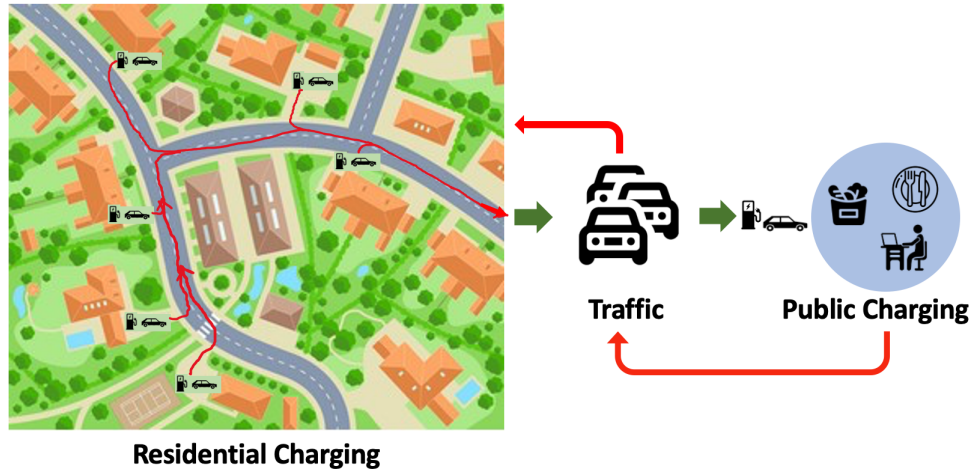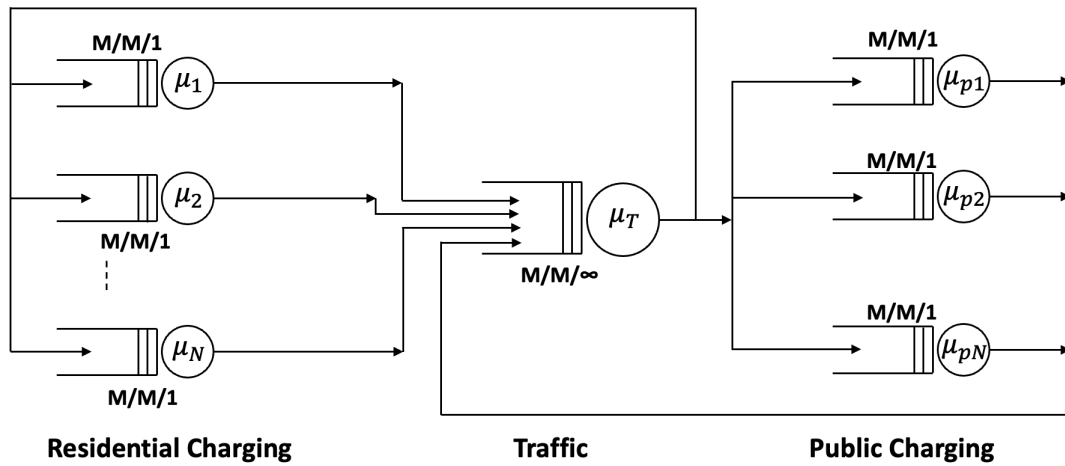
Figure 5.1: Queueing Network model representing a network that consists of multiple charging stations (a) illustration of the queueing network, (b) the equivalent queueing model using M/M/1 and M/M/∞

5.1.1 Performance Measures in Multiple Charging Station Queueing Model

To measure the QoS of the queueing network, we need to calculate the performance measures. Average response time is one of the critical performance measures to be analyzed. By definition, average response time is the time that an EV spends at a charging station (or the traffic network) to be served. This time includes the waiting time (i.e. the time spent waiting in the queue) plus the service time.

The limiting probability for all states of the system has the form:

$$\pi_{(n_1,n_2,...,n_k)} = C \prod_{i=1}^{k} \pi_{n_i} \tag{5.1}$$

$$n_1 + n_2 + ... + n_k = M_{ev} \tag{5.2}$$

k is the number of EVCSs (charger ports) and C represents the normalization factor. To find the average response time we need to solve (5.1). This approach for a network of queueing systems is a challenging process and involves significant computation to determine the normalization factor [68]. Hence, we adopt a more efficient method that directly calculates the average performance values without the need to determine limiting probabilities. This method is called **mean value analysis (MVA)** and it is a recursive approach to finding the average response time in a queueing system.

MVA inherits two strong theorems in queueing theory: 1) The **Arrival theorem** [70] and 2) **Little's Law** described in chapter 3 [71]. The Arrival theorem in a closed Jackson network with $M > 1$ total jobs states that an arrival to server j witnesses a distribution of the number of jobs at each server in the same network with $M - 1$ total jobs. In particular, the mean number of jobs that the arrival sees at server j is $\mathbb{E}[N_j^{(M-1)}]$. The arrival theorem is referred to as the counterpart of PASTA [68].

For single server queueing systems ($M/M/1$), the average response time is calculated by iteratively adding up the number of jobs in the system. Starting at $M = 1$, the average response time is equal to the service rate at j^{th} station denoted by:

$$\mathbb{E}[T_j^{(1)}] = \frac{1}{\mu_j} \tag{5.3}$$

and this is true for all queueing systems in the network. We then use $\mathbb{E}[T_j^{(1)}]$ to calculate $\mathbb{E}[T_j^{(2)}]$ and so forth until we have $\mathbb{E}[T_j^{(M)}]$. These recursive calculations are summarized in the following equations:

$$\mathbb{E}[T_j^{(M)}] = \frac{1}{\mu_j} + \frac{\mathbb{E}[\text{Number at server j as seen by an arrival to j}]}{\mu_j} \tag{5.4}$$

$$= \frac{1}{\mu_j} + \frac{p_j . \lambda^{(M-1)} \mathbb{E}[T_j^{(M-1)}]}{\mu_j} \qquad \text{From Little's Law} \tag{5.5}$$

$$\lambda^{(M)} = \frac{M}{\sum_{j=1}^{N} p_j \mathbb{E}[T_j^{(M)}]} \tag{5.6}$$

To derive the closed form for $\lambda^{(M)}$, the sum of the average number of EVs at all queueing locations is equal to the total population:

$$M = \sum_{j=1}^{k} \mathbb{E}[N_j^{(M)}] \tag{5.7}$$

$$= \sum_{j=1}^{k} \lambda_j^{(M)} \mathbb{E}[T_j^{(M)}] \qquad \text{from Little's Law} \tag{5.8}$$

$$= \sum_{j=1}^{k} p_j \lambda^{(M)} \mathbb{E}[T_j^{(M)}] \tag{5.9}$$

$$= \lambda^{(M)} \sum_{j=1}^{k} p_j \mathbb{E}[T_j^{(M)}] \tag{5.10}$$

$$\longrightarrow \quad \lambda^{(M)} = \frac{M}{\sum_{j=1}^{k} p_j \mathbb{E}[T_j^{(M)}]} \tag{5.11}$$

In the above equations, $\lambda^{(M)}$ denotes the total arrival rate into all queueing systems with (M) jobs in the system. p_j represents the ratio of arrival rate at j^{th} station $(\lambda_j^{(M)})$ over the total arrival rate $\lambda^{(M)}$.

Using the above iterative derivation, the average response time at all locations is derived for a closed Jackson network of $M/M/1$ queueing systems. The full derivation of the above equations is explained in [68, 72].

5.1.2 Approximate MVA Value for Closed Network of EVCS

Closed queueing networks that exhibit a product-form structure, such as Jackson's network, can be analyzed exactly [73]. However, computing the steady-state performance metrics, including server utilization and mean queue lengths, necessitates the calculation of limiting probabilities and normalization constants. Despite its efficiency, obtaining the normalization constant for moderately sized networks can be computationally demanding due to the numerous states involved [73]. Efficient algorithms, including the convolution and MVA methods, have been developed to solve this problem [74, 75].

While the convolution method can be problematic due to numerical difficulties, MVA is frequently utilized to determine closed queueing network performance metrics since it circumvents these problems [73]. However, MVA's time complexity escalates for networks with many service stations, customer classes, and customers in each category. Thus, approximations for performance measures obtained using MVA are necessary. Several approximations have been suggested to decrease the computational complexity of MVA. Chandy and Neuse introduced an approximation for networks with multiple-server stations, which Akyildiz and Bolch subsequently improved [76, 77].

The approximation also helps with defining the performance measures according to control variables that we later use for resource allocation optimiza-

tion problems for the sizing of an EVCS network.

In summary, below are the steps for obtaining an approximate MVA value for performance measures (e.g. average response time):

- Determine a canonical form for the average response time at each EVCS as a function of service rate (and the number of charger ports for networks with $M/M/k$ EVCS).

- Verify that the approximate function follows the disciplined convex programming [78].

Approximation derivation is explained in a case study in the following sections.

5.2   Optimization Problem Formulation

Consider a charging service provider seeking to construct K charger ports at N designated sites. Each charger port adheres to an $M/M/1$ queue, and the ith location possesses k_i ports. Let M_{ev} represent the population of electric vehicles that connect to (or wait in the queue for) residential charger ports before entering the traffic network and subsequently accessing other public fast chargers or waiting in line for charging. The objective is to minimize the charging and investment expenses for all N locations while fulfilling grid-imposed and user-centric performance constraints. Mathematically the optimization problem is

formulated as follows:

$$\min_{k_1 \geq 0, \; k_2 \geq 0, \cdots, k_N \geq 0} \quad \sum_{j=1}^{N} f_{c_j}(k_j.\mu_j) \tag{5.12a}$$

$$s.t. \quad k_i \leq k_i^{max} \tag{5.12b}$$

$$k_1 + k_2 + \cdots + k_N = K \tag{5.12c}$$

$$k_i.\mu_i \leq P_{Tr_i} \tag{5.12d}$$

$$\mathbb{E}[T_i] \leq \mathbb{E}[T_i]^{max} \quad \{i = 1, \cdots, N\} \tag{5.12e}$$

$$\sum_{j=1}^{N} \mathbb{E}[T_j]^{max} = \tau \tag{5.12f}$$

It is assumed that the installation and service costs of charging are of the quadratic function form $(f_{c_j}(k_j.\mu_j) = z_j + y_j.(k_j.\mu_j) + x_j.(k_j.\mu_j)^2)$. The objective function is to minimize the sum of costs at all locations. The decision variables are k_i that are integer variables (i.e. the number of chargers cannot take float values). At each location, there is a cap on the number of chargers to be installed (5.12b). Maximum power consumption at i^{th} location must be less than the transformer feeder rating at that location (5.12d). The response time at each location should be less than a maximum tolerable time (5.12e). The sum of all maximum response times is set to τ (5.12f). This is a strict constraint on the response time and indeed for flexible sizing, τ can be considered as an upper bound in (5.12f).

This problem is a MILP optimization that cannot be solved using standard solvers. Additionally, we have nonlinear function expressions for $\mathbb{E}[T_i]$ using the MVA recursive approach. These nonlinearities make the optimization problem hard to solve and to tackle this issue, we make some assumptions and relax the decision variables and recursive functions to comprise a convex optimization problem [2].

---

[2]The optimization problem should follow the standard form [79]

5.3 Case Study

To illustrate how to solve the optimization problem in (5.12) and the application of closed Jackson's network analysis, we investigate a case study where we model two EVCSs at two locations: 1) residential and 2) public stations with the following assumptions:

- Residential charging ports are available for EV owners to get serviced

- Each residential charger is modeled as an $M/M/1$ with maximum service rate μ_1. It is assumed that there are k_1 of these chargers active for charge delivery in the area.

- The traffic network is modeled as an $M/M/\infty$ with service rate denoted as μ_T.

- Each public charger is modeled as an M/M/1 queue with maximum service rate μ_2 which is assumed to be greater than μ_1. It is assumed that k_2 of these chargers are installed in the second location.

- The population of EV owners is larger than the number of chargers and hence there is a probability of queueing at some charger ports.

- It is assumed that charger ports are not shared and rerouting is neglected.

An EV driver starts their commute at a residential charging location and joins the traffic flow and then connects their EV to a public charger. Fig. 5.2 illustrates this case study for one single EV and single charger port. Indeed the illustration can be extended for k_1 and k_2 number of chargers at residential and public locations, respectively. Case study information is depicted in Table 5.1.

The constraint in (5.12e) is convex based on the results shown in Fig. 5.3. A similar practice is investigated in [73] for multi-server queueing networks. The average response time is then approximated as a function of the number
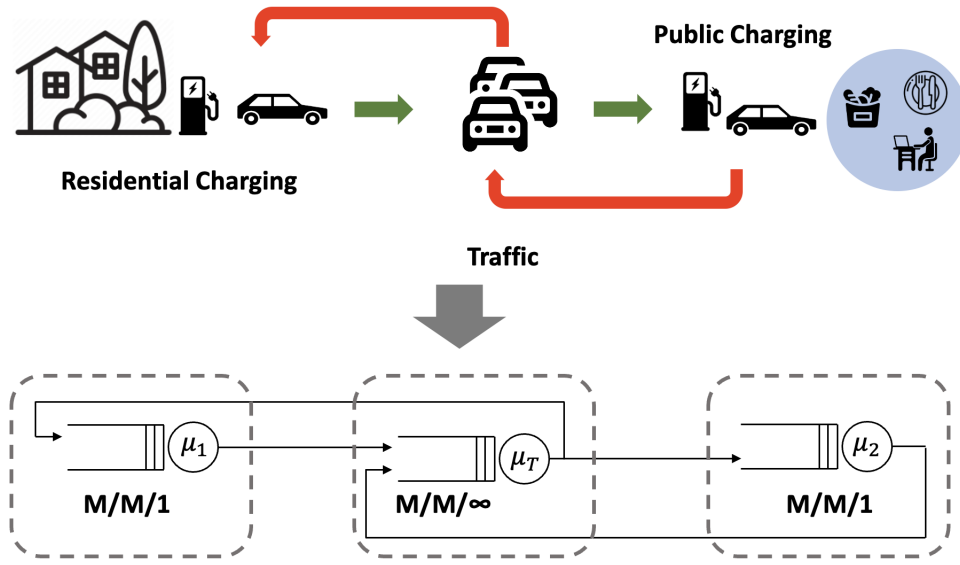
Figure 5.2: EVCS network illustration and the closed queueing network representation

Table 5.1: Data information for the multiple EVCS case study

Parameter	Value
μ_1, μ_2, μ_T	50, 150, 5
k_1^{max}, k_2^{max}	15, 10
P_{Tr_1}, P_{Tr_2}	1000, 6000 [kW]
τ	2.9 [hour]
x_1, y_1, z_1	500, 5, 0.1
x_2, y_2, z_2	5000, 7.5, 0.6

of charger ports and their utilization. In our case, the arrival rate is assumed to be constant and the service rate is variable. Average response time $\mathbb{E}[T_1]$ for different values of μ_1 are shown in Fig. 5.3.

The approximate MVA function is shown to be of the following form:

$$\mathbb{E}[T_1](k_1\mu_1) = \alpha(k_1\mu_1)^\beta \tag{5.13}$$
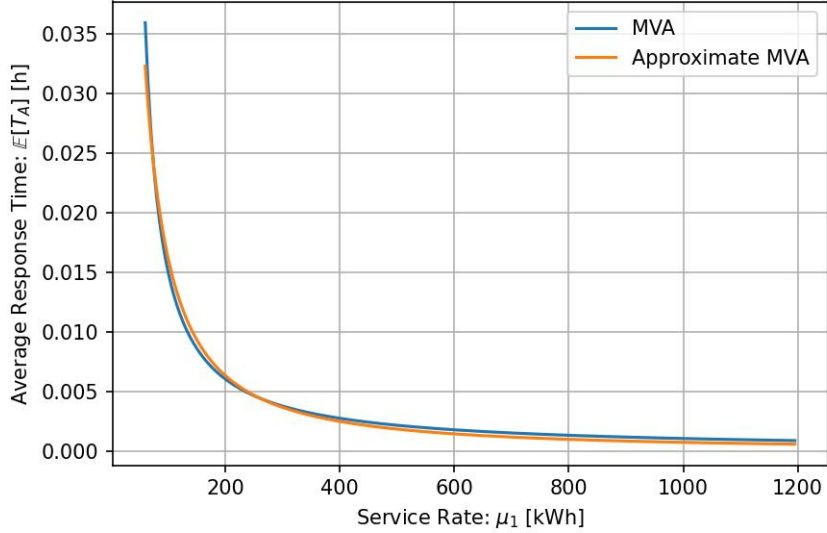
Similar formulation applies for $\mathbb{E}[T_2]$.

Figure 5.3: Location A; Average response time $\mathbb{T}_A$ for various values of μ_A

Using the information in Table 5.1, $\alpha = 159.74$ and $\beta = -2.25$ for location 1. With the approximate function, the optimization problem in 5.12 follows the disciplined convex programming (DCP) and can be readily solved using cvxpy[3] solvers.

The optimum solution $\mu_1^* = 15.64$ and $\mu_2^* = 26.08$ are the results of the optimization problem (assuming $k_1 = k_2 = 1$).

In the next part, we run the optimization problem for multiple $M/M/1$ chargers at residential and public locations with limited transformer capacity.

The objective function is to minimize the installation costs of charger ports at two locations subject to making sure that each charger port does not violate the maximum charge service, the total sum of charger service rates is below the transformer rating capacity (P_{Tr_1} and P_{Tr_2}). The users do not want to wait for a long period of time to charge at either location. This observation comes from the fact that the expectation is to have a constant waiting time at both locations (i.e. $\mathbb{E}[T_1] + \mathbb{E}[T_2] \leq \tau$). The simulation result for this scenario is shown in Fig. 5.4. This figure shows that investing at both locations is a trade-

---

[3]For details on solving cvx programming problems visit `https://www.cvxpy.org/tutorial/dcp/index.html`
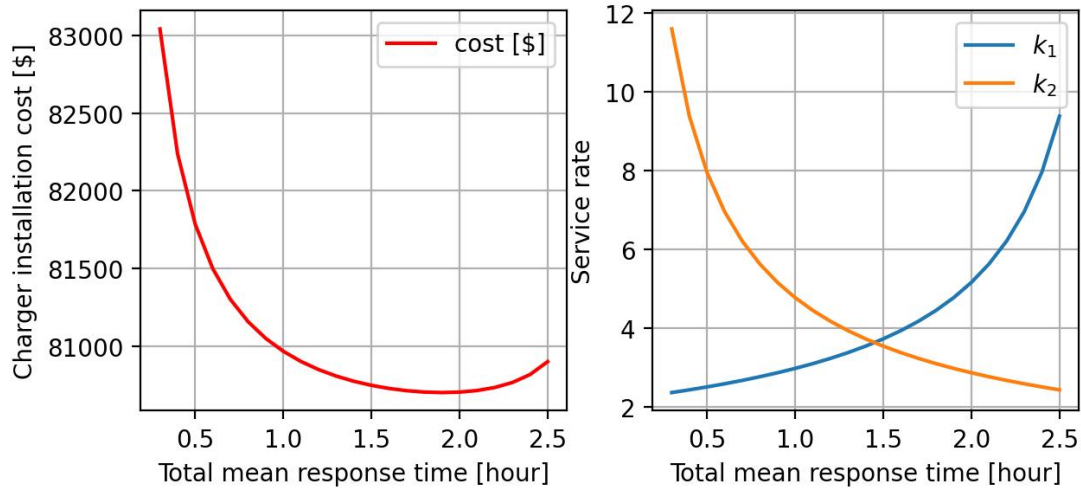
Figure 5.4: Simulation result of the optimization problem explained in 5.12 considering average response time with respect to total charger installation costs and require service rate for locations A and B, respectively.

off; we can have too many expensive chargers installed at the public location and impose costly investment on the EVCS service provider while a moderate expansion at both locations can result in an acceptable response time and thus a response time of approximately 1.5 hours is achieved by installing at least 4 charger ports at either location. The results demonstrate an interesting balance between costs and EV user satisfaction.

Observation   Fig. 5.4 shows the results of solving the optimization problem in (5.12) for various mean response time thresholds. As shown, the charging installation costs vary and has a minimum value of around 2.0 hour. Our observation from the results reveals that for lower response time achievement, higher installation is required in public areas.

Chapter 6

Conclusion & Future Works

6.1 Conclusion

We proposed a robust sizing strategy method to decrease the dependency of EVCS on the main power grid. We investigated a two-fold optimization approach to 1) find the optimal sizing of EVCS to meet service performance requirements (e.g. EV user blocking probability) and 2) provide renewable resource (e.g. solar panel and battery storage) sizing recommendations to support green EVCS and mitigate carbon emissions from fossil fuel-based power grid. We evaluated the sizing strategy on a single EVCS with real-world data. The recommended sizing results are proven to allocate enough resources to meet the seasonal and future growth of EV users for a single EVCS. The final results of reference [30] align with the outcomes of our sizing strategy solution that a combination of level 2 and 3 chargers is more efficient than having level 3 chargers only. The trade-off is the balance between the service provider's profit and EV owners' satisfaction (i.e. a function of the service time etc.).

We modeled a network of charging stations and the traffic flow, and show that Jackson's network in queueing theory is a suitable approach for modeling a network of EVCS and our methodology and solution of modeling a network of EVCS is similar to the one presented in [17] where BCMP network approach

is utilized. We proposed a sizing optimization problem to find the number of charger ports to be installed at multiple locations to meet certain criteria (e.g. service cost budget, service time requirements, etc.). Our result shows a trade-off between the total installation cost and service time. For a very small response time (i.e. user satisfaction), high utilization is required (i.e. service investment cost, a burden on the utility provider). Using some assumptions and relaxations, we turn the complex optimization problem into a convex form that can be readily solved.

Lastly, we address the research questions presented in chapter 1 of this thesis.

- The optimal sizing strategy for EVCSs with on-site PV and BESS systems involves a two-stage sizing assessment. The first stage identifies EVCS sizing options that meet a blocking rate threshold, and the second stage recommends robust sizing alternatives for the PV and BESS systems to minimize reliance on the primary grid. This can be achieved using convex optimization and a Chebyshev inequality for robust sizing. Simulation results indicate that larger sizing of PV and BESS is required for decreased dependence on the main grid, and combining a PV system with a BESS is recommended for optimal performance.

- To optimally size a network of EVCSs, an optimization problem must be established, subject to various constraints such as performance metrics and total costs. Due to the complex nature of this queueing system optimization problem, certain assumptions must be made to obtain a feasible solution. Simulation results indicate that the sizing alternative at each location has a direct impact on performance metrics, leading to an optimal sizing option at each location.

6.2 Future Works Directions

Some aspects of this research work have great potential for improvement. For a single EVCS sizing problem, we incorporated Chebyshev inequality [80] to recommend a robust sizing of solar panels and battery storage. It is worth investigating other probability inequalities such as Chernoff bound as it is an exponentially decreasing upper bound. A comparison of sizing recommendations by incorporating different inequalities has great potential to yield the best robust solution.

An empirical sizing validation of the optimization model for multiple EVCS sizing is necessary and will be performed in future work. We model k charger ports with $M/M/1$ at one location which made the formulation simpler and allowed us to solve the optimization problem. A more rigorous approach would be to model each station as an $M/M/k$ queue which is briefly explained in Appendix B.

Bibliography

[1] Di Wu, Fengdi Guo, Frank R Field III, Robert D De Kleine, Hyung Chul Kim, Timothy J Wallington, and Randolph E Kirchain. Regional heterogeneity in the emissions benefits of electrified and lightweighted light-duty vehicles. *Environmental science & technology*, 53(18):10560–10570, 2019.

[2] Radu Gogoana. *Assessing the viability of level III electric vehicle rapid-charging stations*. PhD thesis, Massachusetts Institute of Technology, 2010.

[3] Trieu T Mai, Paige Jadun, Jeffrey S Logan, Colin A McMillan, Matteo Muratori, Daniel C Steinberg, Laura J Vimmerstedt, Benjamin Haley, Ryan Jones, and Brent Nelson. Electrification futures study: scenarios of electric technology adoption and power consumption for the united states. Technical report, National Renewable Energy Lab.(NREL), Golden, CO (United States), 2018.

[4] Andrew M Mowry and Dharik S Mallapragada. Grid impacts of highway electric vehicle charging and role for mitigation via energy storage. *Energy Policy*, 157:112508, 2021.

[5] Guodong Liu, Madhu Sudhan Chinthavali, Suman Debnath, and Kevin Tomsovic. Optimal sizing of an electric vehicle charging station with integration of pv and energy storage. Technical report, Oak Ridge National Lab.(ORNL), Oak Ridge, TN (United States), 2021.

[6] JA Domínguez-Navarro, R Dufo-López, JM Yusta-Loyo, JS Artal-Sevil,

and JL Bernal-Agustín. Design of an electric vehicle fast-charging station with integration of renewable energy and storage systems. *International Journal of Electrical Power & Energy Systems*, 105:46–58, 2019.

[7] Islam Safak Bayram, Michael Devetsikiotis, and Raka Jovanovic. Optimal design of electric vehicle charging stations for commercial premises. *International Journal of Energy Research*, 46(8):10040–10051, 2022.

[8] Yongmin Zhang, Pengcheng You, and Lin Cai. Optimal charging scheduling by pricing for ev charging station with dual charging modes. *IEEE Transactions on Intelligent Transportation Systems*, 20(9):3386–3396, 2018.

[9] Arnab Pal, Aniruddha Bhattacharya, and Ajoy Kumar Chakraborty. Placement of public fast-charging station and solar distributed generation with battery energy storage in distribution network considering uncertainties and traffic congestion. *Journal of Energy Storage*, 41:102939, 2021.

[10] Emin Ucer, Işıl Koyuncu, Mithat C Kisacikoglu, Mesut Yavuz, Andrew Meintz, and Clément Rames. Modeling and analysis of a fast charging station and evaluation of service quality for electric vehicles. *IEEE Transactions on Transportation Electrification*, 5(1):215–225, 2019.

[11] Nikhil Kumar, Tushar Kumar, Savita Nema, and Tripta Thakur. A comprehensive planning framework for electric vehicles fast charging station assisted by solar and battery based on queueing theory and non-dominated sorting genetic algorithm-ii in a co-ordinated transportation and power network. *Journal of Energy Storage*, 49:104180, 2022.

[12] Mohammadhadi Rouhani, Mohammad Mohammadi, and Amin Kargarian. Parzen window density estimator-based probabilistic power flow with correlated uncertainties. *IEEE Transactions on Sustainable Energy*, 7(3): 1170–1181, 2016.

[13] Hongcai Zhang, Scott Moura, Zechun Hu, Wei Qi, and Yonghua Song. Joint pev charging station and distributed pv generation planning. In *2017 IEEE power & energy society general meeting*, pages 1–5. IEEE, 2017.

[14] Dingtong Yang, Navjyoth JS Sarma, Michael F Hyland, and R Jayakrishnan. Dynamic modeling and real-time management of a system of ev fast-charging stations. *Transportation Research Part C: Emerging Technologies*, 128:103186, 2021.

[15] Cuiyu Kong, Raka Jovanovic, Islam Safak Bayram, and Michael Devetsikiotis. A hierarchical optimization model for a network of electric vehicle charging stations. *Energies*, 10(5):675, 2017.

[16] Rachad Atat, Muhammad Ismail, Erchin Serpedin, and Thomas Overbye. Dynamic joint allocation of ev charging stations and dgs in spatio-temporal expanding grids. *IEEE Access*, 8:7280–7294, 2020.

[17] Hao Liang, Isha Sharma, Weihua Zhuang, and Kankar Bhattacharya. Plug-in electric vehicle charging demand estimation based on queueing network analysis. In *2014 IEEE PES General Meeting— Conference & Exposition*, pages 1–5. IEEE, 2014.

[18] Lae Yeop Lee, Won Seok Choi, and Seong Gon Choi. Investment cost minimization of autonomous-electric vehicles based on queueing model. In *2022 24th International Conference on Advanced Communication Technology (ICACT)*, pages 172–178. IEEE, 2022.

[19] Xiaoqi Tan, Bo Sun, Yuan Wu, and Danny HK Tsang. Asymptotic performance evaluation of battery swapping and charging station for electric vehicles. *Performance Evaluation*, 119:43–57, 2018.

[20] Sanzhong Bai, Du Yu, and Srdjan Lukic. Optimum design of an ev/phev

charging station with dc bus and storage system. In *2010 IEEE Energy Conversion Congress and Exposition*, pages 1178–1184. IEEE, 2010.

[21] Xian Zhang, Ka Wing Chan, Hairong Li, Huaizhi Wang, Jing Qiu, and Guibin Wang. Deep-learning-based probabilistic forecasting of electric vehicle charging load with a novel queuing model. *IEEE transactions on cybernetics*, 51(6):3157–3170, 2020.

[22] Insights into future mobility mit, accessed: 12.1.2020. URL `https://energy.mit.edu/research/mobilityofthefuture/`.

[23] Mustafa Ammous, Syrine Belakaria, Sameh Sorour, and Ahmed Abdel-Rahim. Optimal cloud-based routing with in-route charging of mobility-on-demand electric vehicles. *IEEE Transactions on Intelligent Transportation Systems*, 20(7):2510–2522, 2018.

[24] Mohammadreza Kavianipour, Fatemeh Fakhrmoosavi, Harprinderjot Singh, Mehrnaz Ghamami, Ali Zockaie, Yanfeng Ouyang, and Robert Jackson. Electric vehicle fast charging infrastructure planning in urban networks considering daily travel and charging behavior. *Transportation Research Part D: Transport and Environment*, 93:102769, 2021.

[25] Andreas Seitaridis, Emmanouil S Rigas, Nick Bassiliades, and Sarvapali D Ramchurn. An agent-based negotiation scheme for the distribution of electric vehicles across a set of charging stations. *Simulation Modelling Practice and Theory*, 100:102040, 2020.

[26] Zhipeng Liu, Fushuan Wen, and Gerard Ledwich. Optimal planning of electric-vehicle charging stations in distribution systems. *IEEE transactions on power delivery*, 28(1):102–110, 2012.

[27] Guibin Wang, Zhao Xu, Fushuan Wen, and Kit Po Wong. Traffic-

constrained multiobjective planning of electric-vehicle charging stations. *IEEE Transactions on Power Delivery*, 28(4):2363–2372, 2013.

[28] I Safak Bayram, George Michailidis, Michael Devetsikiotis, and Fabrizio Granelli. Electric power allocation in a network of fast charging stations. *IEEE Journal on Selected Areas in Communications*, 31(7):1235–1246, 2013.

[29] Fei Xie, Changzheng Liu, Shengyin Li, Zhenhong Lin, and Yongxi Huang. Long-term strategic planning of inter-city fast charging infrastructure for battery electric vehicles. *Transportation Research Part E: Logistics and Transportation Review*, 109:261–276, 2018.

[30] Xiaomin Xi, Ramteen Sioshansi, and Vincenzo Marano. Simulation–optimization model for location of a public electric vehicle charging infrastructure. *Transportation Research Part D: Transport and Environment*, 22:60–69, 2013.

[31] Mohannad Kabli, Md Abdul Quddus, Sarah G Nurre, Mohammad Marufuzzaman, and John M Usher. A stochastic programming approach for electric vehicle charging station expansion plans. *International Journal of Production Economics*, 220:107461, 2020.

[32] Islam Safak Bayram, Michael Devetsikiotis, and Raka Jovanovic. Optimal design of electric vehicle charging stations for commercial premises. *International Journal of Energy Research*, 2021.

[33] Forest Baskett, K Mani Chandy, Richard R Muntz, and Fernando G Palacios. Open, closed, and mixed networks of queues with different classes of customers. *Journal of the ACM (JACM)*, 22(2):248–260, 1975.

[34] Yue Xiang, Junyong Liu, Ran Li, Furong Li, Chenghong Gu, and Shuoya Tang. Economic planning of electric vehicle charging stations considering

traffic constraints and load profile templates. *Applied Energy*, 178:647–659, 2016.

[35] Xiaohong Dong, Yunfei Mu, Hongjie Jia, Jianzhong Wu, and Xiaodan Yu. Planning of fast ev charging stations on a round freeway. *IEEE Transactions on Sustainable Energy*, 7(4):1452–1461, 2016.

[36] Samantha J Gunter, Khurram K Afridi, and David J Perreault. Optimal design of grid-connected pev charging systems with integrated distributed resources. *IEEE Transactions on Smart Grid*, 4(2):956–967, 2013.

[37] Dan Xiao, Shi An, Hua Cai, Jian Wang, and Haiming Cai. An optimization model for electric vehicle charging infrastructure planning considering queuing behavior with finite queue length. *Journal of Energy Storage*, 29: 101317, 2020.

[38] Jie Yang, Jing Dong, and Liang Hu. A data-driven optimization-based approach for siting and sizing of electric taxi charging stations. *Transportation Research Part C: Emerging Technologies*, 77:462–477, 2017.

[39] Yu Ru et al. Storage size determination for grid-connected photovoltaic systems. *IEEE Transactions on Sustainable Energy*, 4(1):68–81, 2012.

[40] Jean-Michel Clairand et al. Power generation planning of galapagos' microgrid considering electric vehicles and induction stoves. *IEEE Transactions on Sustainable Energy*, 10(4):1916–1926, 2018.

[41] Indrajit Das and Claudio A Cañizares. Renewable energy integration in diesel-based microgrids at the canadian arctic. *Proc. IEEE*, 107(9):1838–1856, 2019.

[42] Yashar Ghiassi-Farrokhfal et al. Optimal design of solar PV farms with storage. *IEEE Transactions on Sustainable Energy*, 6(4):1586–1593, 2015.

[43] Hongcai Zhang, Scott J Moura, Zechun Hu, Wei Qi, and Yonghua Song. Joint pev charging network and distributed pv generation planning based on accelerated generalized benders decomposition. *IEEE transactions on transportation electrification*, 4(3):789–803, 2018.

[44] Ke Zhang, Yuming Mao, Supeng Leng, Yan Zhang, Stein Gjessing, and Danny HK Tsang. Platoon-based electric vehicles charging with renewable energy supply: A queuing analytical model. In *2016 IEEE International Conference on Communications (ICC)*, pages 1–6. IEEE, 2016.

[45] Juliette Ugirumurera and Zygmunt J Haas. Optimal capacity sizing for completely green charging systems for electric vehicles. *IEEE Transactions on Transportation Electrification*, 3(3):565–577, 2017.

[46] Mohammadhadi Rouhani, Omid Ardakanian, and Petr Musilek. Robust sizing of solar-powered charging stationwith co-located energy storage. *Subitted to IEEE Power & Energy Society General Meeting (PES-GM)*, 2022.

[47] E Pashajavid and MA Golkar. Optimal placement and sizing of plug in electric vehicles charging stations within distribution networks with high penetration of photovoltaic panels. *Journal of Renewable and Sustainable Energy*, 5(5):053126, 2013.

[48] Madathodika Asna, Hussain Shareef, Prasanthi Achikkulath, Hazlie Mokhlis, Rachid Errouissi, and Addy Wahyudie. Analysis of an optimal planning model for electric vehicle fast-charging stations in al ain city, united arab emirates. *IEEE Access*, 9:73678–73694, 2021.

[49] Alireza Khaksari, Georgios Tsaousoglou, Prodromos Makris, Konstantinos Steriotis, Nikolaos Efthymiopoulos, and Emmanouel Varvarigos. Sizing of electric vehicle charging stations with smart charging capabilities and

quality of service requirements. *Sustainable Cities and Society*, 70:102872, 2021.

[50] Pilar Meneses de Quevedo, Gregorio Muñoz-Delgado, and Javier Contreras. Impact of electric vehicles on the expansion planning of distribution systems considering renewable energy, storage, and charging stations. *IEEE Transactions on Smart Grid*, 10(1):794–804, 2017.

[51] Xin Li, Luiz AC Lopes, and Sheldon S Williamson. On the suitability of plug-in hybrid electric vehicle (phev) charging infrastructures based on wind and solar energy. In *2009 IEEE Power & Energy Society General Meeting*, pages 1–8. IEEE, 2009.

[52] Stephen Lee, Srinivasan Iyengar, David Irwin, and Prashant Shenoy. Shared solar-powered ev charging stations: Feasibility and benefits. In *2016 Seventh International Green and Sustainable Computing Conference (IGSC)*, pages 1–8. IEEE, 2016.

[53] Zachary Lee et al. ACN-Data: Analysis and applications of an open EV charging dataset. In *Proc 10th ACM International Conference on Future Energy Systems*, pages 139–149, 2019.

[54] Yvenn Amara-Ouali, Yannig Goude, Pascal Massart, Jean-Michel Poggi, and Hui Yan. A review of electric vehicle load open data and models. *Energies*, 14(8):2233, 2021.

[55] Zonggen Yi and Peter H Bauer. Energy consumption model and charging station placement for electric vehicles. In *Smartgreens*, pages 150–156, 2014.

[56] Dario Pevec, Jurica Babic, Martin A Kayser, Arthur Carvalho, Yashar Ghiassi-Farrokhfal, and Vedran Podobnik. A data-driven statistical ap-

proach for extending electric vehicle charging infrastructure. *International journal of energy research*, 42(9):3102–3120, 2018.

[57] Hao Tu, Hao Feng, Srdjan Srdic, and Srdjan Lukic. Extreme fast charging of electric vehicles: A technology overview. *IEEE Transactions on Transportation Electrification*, 5(4):861–878, 2019.

[58] Qiang Yang et al. Optimal sizing of PEV fast charging stations with Markovian demand characterization. *IEEE Transactions on Smart Grid*, 10(4):4457–4466, 2018.

[59] Sajad Esmailirad, Ali Ghiasian, and Abdorreza Rabiee. An extended m/m/k/k queueing model to analyze the profit of a multiservice electric vehicle charging station. *IEEE Transactions on Vehicular Technology*, 70 (4):3007–3016, 2021.

[60] Ralph L Disney and Dieter König. Queueing networks: A survey of their random processes. *SIAM review*, 27(3):335–403, 1985.

[61] Fiodar Kazhamiaka, Yashar Ghiassi-Farrokhfal, Srinivasan Keshav, and Catherine Rosenberg. Comparison of different approaches for solar pv and storage sizing. *IEEE Transactions on Sustainable Computing*, 7(3): 499–511, 2019.

[62] John Saw et al. Chebyshev inequality with estimated mean and variance. *The American Statistician*, 38(2):130–132, 1984.

[63] Mostafa F Shaaban, Yasser M Atwa, and Ehab F El-Saadany. Pevs modeling and impacts mitigation in distribution networks. *IEEE Transactions on Power Systems*, 28(2):1122–1131, 2012.

[64] Xu Wang, Mohammad Shahidehpour, Chuanwen Jiang, and Zhiyi Li. Coordinated planning strategy for electric vehicle charging stations and cou-

pled traffic-electric networks. *IEEE Transactions on Power Systems*, 34 (1):268–279, 2018.

[65] Islam Safak Bayram, Ali Tajer, Mohamed Abdallah, and Khalid Qaraqe. Capacity planning frameworks for electric vehicle charging stations with multiclass customers. *IEEE Transactions on Smart Grid*, 6(4):1934–1943, 2015.

[66] Meina Zheng, Feng Liu, Xiucheng Guo, and Xinyue Lei. Assessing the distribution of commuting trips and jobs-housing balance using smart card data: A case study of nanjing, china. *Sustainability*, 11(19):5346, 2019.

[67] Jingqiu Guo, Yong Zhang, Xinyao Chen, Saleh Yousefi, Chenyu Guo, and Yibing Wang. Spatial stochastic vehicle traffic modeling for vanets. *IEEE Transactions on Intelligent Transportation Systems*, 19(2):416–425, 2017.

[68] Mor Harchol-Balter. *Performance modeling and design of computer systems: queueing theory in action*. Cambridge University Press, 2013.

[69] Yonathan Bard. Some extensions to multiclass queueing network analysis. In *Proceedings of the Third International Symposium on Modelling and Performance Evaluation of Computer Systems: Performance of Computer Systems*, pages 51–62, 1979.

[70] Stephen S Lavenberg and Martin Reiser. Stationary state probabilities at arrival instants for closed queueing networks with multiple types of customers. *Journal of Applied Probability*, 17(4):1048–1061, 1980.

[71] John DC Little. A proof for the queuing formula: L= λ w. *Operations research*, 9(3):383–387, 1961.

[72] Sanjay K Bose. *An introduction to queueing systems*. Springer Science & Business Media, 2013.

[73] Rajan Suri, Sushanta Sahu, and Mary Vernon. Approximate mean value analysis for closed queuing networks with multiple-server stations. In *Proceedings of the 2007 Industrial Engineering Research Conference*, pages 1–6, 2007.

[74] Jeffrey P Buzen. Computational algorithms for closed queueing networks with exponential servers. *Communications of the ACM*, 16(9):527–531, 1973.

[75] Martin Reiser and Stephen S Lavenberg. Mean-value analysis of closed multichain queuing networks. *Journal of the ACM (JACM)*, 27(2):313–322, 1980.

[76] Doug Neuse and K Chandy. Scat: A heuristic algorithm for queueing network models of computing systems. In *Proceedings of the 1981 ACM SIGMETRICS conference on Measurement and modeling of computer systems*, pages 59–79, 1981.

[77] Ian F Akyildiz and Gunter Bolch. Mean value analysis approximation for multiple server queueing networks. *Performance Evaluation*, 8(2):77–91, 1988.

[78] Michael Grant, Stephen Boyd, and Yinyu Ye. Disciplined convex programming. In *Global optimization*, pages 155–210. Springer, 2006.

[79] Stephen Boyd, Stephen P Boyd, and Lieven Vandenberghe. *Convex optimization*. Cambridge university press, 2004.

[80] John G Saw, Mark CK Yang, and Tse Chin Mo. Chebyshev inequality with estimated mean and variance. *The American Statistician*, 38(2):130–132, 1984.

Appendix A

CTMC Model of an EVCS with two types of chargers

This appendix provides a detailed explanation of how the CTMC model is derived for an EVCS with two charger types (level 2 and level 3).

Consider the design of a charging station with two levels of chargers, denoted as level 1 and level 2. Let the number of chargers at level 1 and level 2 be represented by A and B, respectively, with service rates denoted as μ_1 and μ_2. It is assumed that $\mu_2 > \mu_1$, indicating that level 2 chargers provide a higher service rate. When the charging station is unoccupied, A level 2 chargers are prioritized to be occupied, and for the $A + 1^{th}$ electric vehicle (EV), B level 1 charger ports are available.

The arrival rate of EVs is modeled as an independent Poisson process with an expected arrival rate of λ. The inter-arrival time of EVs follows an exponential distribution, which is an appropriate assumption to model a continuous Markov chain for this EV charging system. The state transition of the system, as a function of the number of EVs present, is illustrated in Figure A.1, following Kendall's notation of $M/M/k/k$ where $k = A + B$.

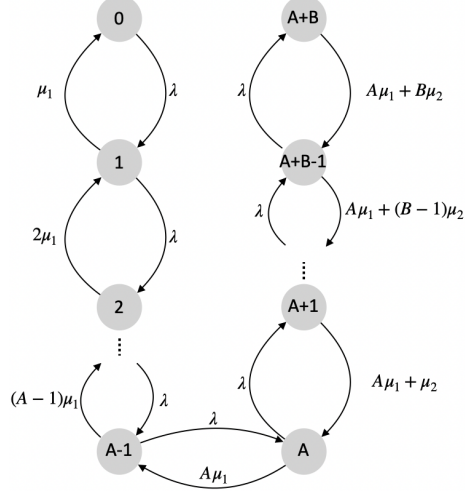We denote the limiting probabilities for each state i in the EVCS queue system as π_i.

Figure A.1: Continous-time Markov Chain representation of M/M/k/k based EVSE states with 'A' level 2 and 'B' level 1 chargers.

We show that the EVCS system is time-reversible and irreducible and considering the summation of all limiting probabilities is 1 we then determine π_i for $i \in \{0, 1, ..., k\}$.

From Fig. A.1, we can write the following balancing equations for states:

$$\lambda \pi_0 = \mu_1 \pi_1$$

$$\lambda \pi_1 = 2\mu_1 \pi_2$$

$$...$$

$$\lambda \pi_{A-1} = A\mu_1 \pi_A$$

$$\lambda \pi_A = (A\mu_1 + \mu_2)\pi_{A+1}$$

$$...$$

$$\lambda \pi_{A+B-2} = (A\mu_1 + (B-1)\mu_2)\pi_{A+B-1}$$

$$\lambda \pi_{A+B-1} = (A\mu_1 + B\mu_2)\pi_{A+B} \tag{A.1}$$

Hence, the limiting probability π_i can then be generally determined as fol-

lows:

$$
\pi_i =
\begin{cases}
\dfrac{\lambda^i}{i!\,\mu_1^i}\pi_0 & 0 \le i \le A \\[4ex]
\dfrac{\lambda^i}{A!\,\mu_1^A \prod_{j=1}^{i-A}(A\mu_1 + j\mu_2)}\pi_0 & A < i \le A + B
\end{cases}
\tag{A.2}
$$

where π_0 is solved from the following equation:

$$
\sum_{i=0}^{A+B} \pi_i = 1
\tag{A.3}
$$

$$
\pi_0 = \left[\sum_{i=0}^{A} \frac{\lambda^i}{i!\,\mu_1^i} + \sum_{i=A+1}^{A+B} \frac{\lambda^i}{A!\,\mu_1^A \prod_{j=1}^{i-A}(A\mu_1 + j\mu_2)}\right]^{-1}
\tag{A.4}
$$

The average number of EVs at the charging station denoted as $\overline{E}_N$ is then determined as

$$
\mathbb{E}[N] = \sum_{i=0}^{A+B} i\pi_i
$$

$$
= \pi_0\left[\sum_{i=0}^{A} \frac{\lambda^i}{(i-1)!\,\mu_1^i} + \frac{1}{A!\,\mu_1^A}\sum_{i=A+1}^{A+B} \frac{i\lambda^i}{\prod_{j=1}^{i-A}(A\mu_1 + j\mu_2)}\right]
\tag{A.5}
$$

Using little's law the average waiting time $\overline{E}_T$ is then determined as follows

$$
\mathbb{E}[T] = \frac{\mathbb{E}[N]}{\lambda}
\tag{A.6}
$$

An interesting problem to be solved for this type of queueing system is to minimize the blocking probability denoted by $P_{blk} = \pi_{A+B}$ subject to certain constraints on performance measures.

Appendix B

Performance Analysis of Multiple Charging Stations with Multi-Charging Ports

This appendix is dedicated to providing a more comprehensive derivation of the average response time using MVA for closed networks with $M/M/k_i$ EVCS and road network.
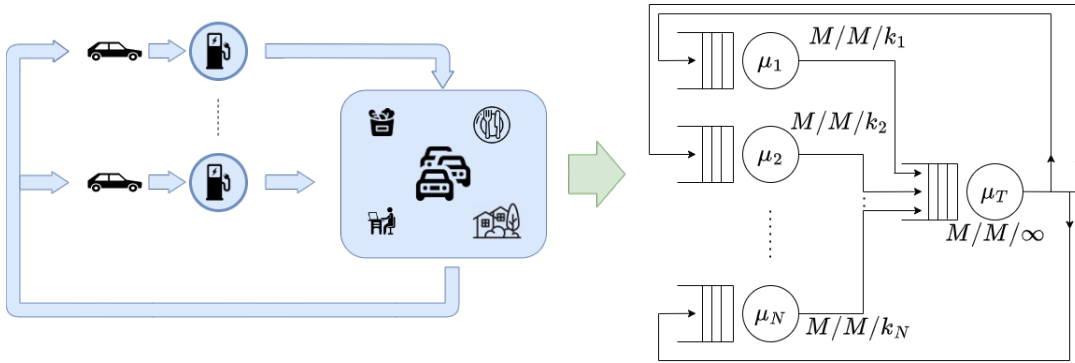

Figure B.1: Network of EVCS modeled as $M/M/k$

As shown in Fig. B.1, we are interested in calculating the average response time for stations with multiple charging ports (i.e. $M/M/k_i$).

The derivation for $M/M/k_i$ is briefly explained in [72] and in detail for

multiclass users in [77]. In [73], an approximation method is used to find the average response time for queueing systems of multiple servers, however, the computation of limiting probabilities has not been defined, and nor has the evaluation of the proposed approximation method is tested for general networks.

Here, we explain and provide the results for average response time for charging stations with multiple charger ports (i.e. $M/M/k_i$ queueing model). The full derivation is explained in Appendix C.

The average response time for queueing systems with infinite server capacity and queueing systems with multiple servers is determined as follows:

$$
\mathbb{E}[T_j^{(m)}] = \begin{cases} \frac{1}{\mu_j} & \text{Infinite Server} \\ \frac{1}{\mu_j} + \frac{\mathbb{E}[(T)_j^{(m-1)}] \cdot p_j \lambda^{(m-1)} + S_j^{(m)}}{\mu_j} & \text{Multi server FCFS} \end{cases} \quad \text{(B.1)}
$$

where p_j and $\lambda^{(m-1)}$ are calculated similar to the single server queues. $S_j^{(m)}$ is defined as

$$
S_j^{(m)} = \sum_{k=1}^{c_j-1} (c_j - k) \mathcal{P}_j(k-1, m-1) \quad \text{(B.2)}
$$

$\mathcal{P}_j(k, m)$ is the marginal probability of k jobs at station j given population m. This probability is determined as follows

$$
\mathcal{P}_j(k, m) = \begin{cases} 1 - \sum_{i=1}^{\mathbf{K}} \mathcal{P}_j(i, m) & \text{for k = 0} \\ \frac{\lambda^{(m)} \mathcal{P}_j(k-1, m-1)}{\mu_j} & \text{for k = 1,..., } (c_k - 1) \end{cases} \quad \text{(B.3)}
$$

Using above recursive equations, average response time for $\mathbf{K}$ multiserver charging stations (j=1,...,$\mathbf{K}$), each charging station with c_j charging port and the total network population of m EVs (m=1,...,M). The recursive function terminates when $m = M$.

Appendix C

Closed Network of Multiple Charging Stations

This appendix explains in detail the derivation of a closed queueing network of charging stations with multiple classes of EVs.

A network of charging stations taking into account multi-class types of EVs present in the traffic network with a closed queueing Jackson's network with a finite population. The Arrival Instant Distribution Theorem states that a class-r EV, arriving at station i in the system with population K, sees the system with population $(K - 1_r)$ in equilibrium. From the Arrival Instant Distribution Theorem the mean response time of a class-r job in station i, $\bar{t}_{ir}(k)$, is computed. The algorithm for the MVA computation is shown in 1. Using Little's Law, the system throughput for each class, $\lambda_r(k)$, and the mean number of jobs, $\bar{k}_{ir}(k)$, are obtained. The general algorithm for classical mean value analysis with multiple server stations is given below.

Table C.1: Table of notations for Algorithm 1

Notation	Definition
$\mathcal{M}$	the total network EV population
M_r	the EV population in class r
K	total number of charging stations in the network
k_i	the number of charger ports at charging station i
R	total number of EV classes
μ_{ir}	the mean charge service rate of a class r EV at charging station i
$\mathbf{m}$	the job vectors denoted by $(m_1, m_2, ..., m_R)$
$\mathbf{m} - 1_r$	the job vector $\mathbf{m}$ with one charge demand removed from class r
$p_{ir;\ js}$	the transition probability of a class r charge demand at station i to class s at station j
$e_{ir}{}^*$	mean number of visits a class-r job makes to station i
$x_{ir} = e_{ir}/\mu_{ir}$	relative utilization of station i for class r jobs
$\bar{T}_{ir}$	mean response time for a class-r job at station i, given EV population $\mathbf{m}$
$\bar{m}_{ir}(\mathbf{m})$	the mean number of jobs at station i in class r, given population $\mathbf{m}$;
$\lambda_r(\mathbf{m})$	the total throughput of class r, given population $\mathbf{m}$
$p_i(j|\mathbf{m})$	marginal probability of j jobs at station i, given population $\mathbf{m}$

$^*e_{ir} = \sum_{j=1}^{K} \sum_{s=1}^{R} e_{js} p_{js;ir}$

Algorithm 1 Calculate Average Response Time using MVA [77]

Initialise:

$$\bar{m}_{ir}(\mathbf{0}) = 0 \forall i = 1, ..., K \ r = 1, ..., R$$
$$p_i(j|\mathbf{0}) = 0 \forall j = 1, ..., (k_i - 1)$$
$$p_i(0|\mathbf{0}) = 1$$

for $\mathbf{m} = 0$ to $\mathcal{M}$ **do**
   for stations $i = 1$ to K and $r = 1$ to R **do**
      $\bar{T}_{ir}(\mathbf{m}) = \dfrac{1}{\mu_{ir}k_i}[1 + \sum_{s=1}^{R} \bar{m}_{is}(\mathbf{m} - 1_r) + \sum_{j=1}^{k_i-j} p_i(j - 1|\mathbf{m} - 1_r)]$
      $\lambda_r(\mathbf{m}) = \dfrac{m_r}{\sum_{i=1}^{K} e_{ir}\bar{T}_{ir}(\mathbf{m})}$
      $\bar{m}_{ir}(\mathbf{m}) = e_{ir}\lambda_r(\mathbf{m})\bar{T}_{ir}(\mathbf{m})$
      for $j = 1$ to $k_i - 1$ **do**
         $p_i(j|\mathbf{m}) = \dfrac{1}{j}[\sum_{r=1}^{R} x_{ir}\lambda_r(\mathbf{m})p_i(j - 1|\mathbf{m} - 1_r)]$
      end for
      $p_i(0|\mathbf{m}) = 1 - \dfrac{1}{m_i}[\sum_{r=1}^{R} x_{ir}\lambda_r(\mathbf{m}) + \sum_{j=1}^{k_i-1}(k_i - j)p_i(j|\mathbf{m})]$
   end for
end for